CHAoAoaSaoaOAOaSOAas

an independant inquiry in at least two parts

By Dan Ernst
Fall 1993

For Dr. Marsden
Math 189?

This project's presentation will be divided into two main categories; the experimental, and the non-experimental research. The experimental section is itself divided into roughly four seperate experiments. I looked at a simple sin wave simulation of a time-series, the logistic map, the Henon mapping, and finally a simple circuit's response to a driving oscillation. The research I did investigates the relation between chaos theory and observed time series EEG. In addition to all the research, a good deal of my time this semester was spent just acquiring a basic understanding of the subject from a simple mathmatical perspective. Some of the texts I found most helpful were:

Abraham, Ralph; Shaw, Chris; Dynamics: the Geometry of Behavior; vol 1-4; UC Santa Cruz, Ariel Press, 1988.

Berge, Pierre; Order within Chaos; Hermann, Paris, 1984.

Ruelle, David; Chaotic evolution and strange attractors; Cambridge University Press; 1989.

Peitgen, Jurgens and Saupe;Chaos and Fractals, new frontiers of Science; Springer-Verlag; 1992.

This project was undoubtedly one of the most exciting and stimulating in my academic career. I thank you again Dr. Marsden for giving me the opportunity of studying this subject.

Dan Ernst
714-8546597
igy@soda

PART I

Experimental Section

Abstract:

This experiment looks at the similarities in systems that exhibit chaotic behavior. We determine the topological equivalence of the bifurcation diagrams of two mathematical and one physical system that follow the 'period doubling route to chaos'. The Feigenbaum number calculated from observation was less than .21% off from the accepted value.

Introduction:

Historically, Physics has been concerned with simplicity. Physics seeks to understand from first principles, that is from the most basic ground up. With the advent of chaos theory, suddenly complexity has become a focus. The belief in the possibility of an understanding of phenomenon from first principles alone was most famously vocalized in LaPlace's comment, "when we know the present precisely, we can know the future."

Heisenberg challenged this determinism from one end, pointing out that the assumption of the possibility of ever knowing the present precisely is false. There is a limit to the precision with which we can specify the state of a system, thus LaPlace's determinism is fundamentally flawed.

Lorentz, Ruellle, and those involved in the beginnings of Chaos theory attack from the other end. There are systems in which the propagation of error increases exponentially. That is, the error in the signal measurement rapidly increases beyond the proportion of the original signal, and thus loses any measurable connection to its past history. This gets at the point that determinism and predictability are not equivalent. A system's

behavior can be completely determined by a simple process, yet the simplicity of this process may not be reflected in a simple result.

Theory:

Chaos theory directly relates to Physics in the study of the dynamics of dissipative systems. If a system is dissipative, then its trajectory in phase space converges to an attractor. There are three types of simple attractors. The simplest is a point attractor, where all trajectories in the basin of attraction converge to a particular point. By 'basin of attraction', I mean the set of all initial conditions that give rise to a trajectory that converges towards the attractor. The second type of attractor is the limit cycle, where the trajectory is periodic in time. The Fourier spectrum of a limit cycle is one fundamental frequency spike with the possibility of harmonics of that frequency (depending on the shape of the time series' waveform). The third type of simple attractor is the torus of dimension r, where r is the number of independent fundamental frequencies present in the signal.

What Lorenz discovered is that there is a fourth type of attractor, the 'strange attractor'. 'Strange attractors', as termed by Ruelle, are characterized by sensitivity to initial conditions (s.i.c.). That is, two initially close trajectories in phase space diverge rapidly. Regardless of how arbitrarily close any two initial positions are, their behavior as projected far into the future can be radically different, and in fact completely uncorrelated. Furthermore, rather than form a finite series of discrete points, a single trajectory's projection onto a strobe

plane (Poincare' section) will fill a broad region that we call a strange attractor. This is to say, the trajectory is not periodic. If we let the system run an infinite length of time, it will produce an infinite number of different points all along the strange attractor. This is why we can say that the trajectory fills the region; for any arbitrary point on the attractor, our trajectory will either pass through it or get infinitely close. If the trajectory is aperiodic in this way, "if the power spectrum has a continuous part", then we have what Berge' defines as chaotic behavior.

Since the system is a completely determinate one, we know that two different trajectories will never cross. But then how is it possible, that every trajectory fills the region we call the 'strange attractor'? The best way to visualize this is to look at the Cantor set, figure T1. The Poincare' section of two trajectories can be seen as two inter-embedded Cantor sets. When we project these sets over an infinite amount of time, each fills the entire region without ever overlapping. This type of fractal structure is precisely what we observe in the Henon map that is the second part of my experiment.

Along with qualitative properties such as the type of self-similarity implicit in fractal structures observed here, and s.i.c., there are also quantitative properties of chaotic behavior that appear to be universal. Michell Feigenbaum observed that there are universal numbers delta, δ , and epsilon, ε , that characterize the bifurcation diagrams of systems that follow the period doubling route to chaos.

FIG T1: CANTOR SET AND SIMILARITY TO MAPPING OF HENON EQN'S

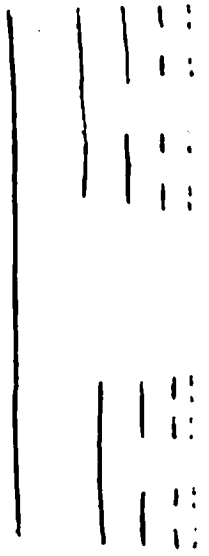

EACH ITERATION TAKES OUT THE MIDDLE THIRD OF THE PREVIOUS SEGMENT

CANTOR SET

HENON MAPPINGS

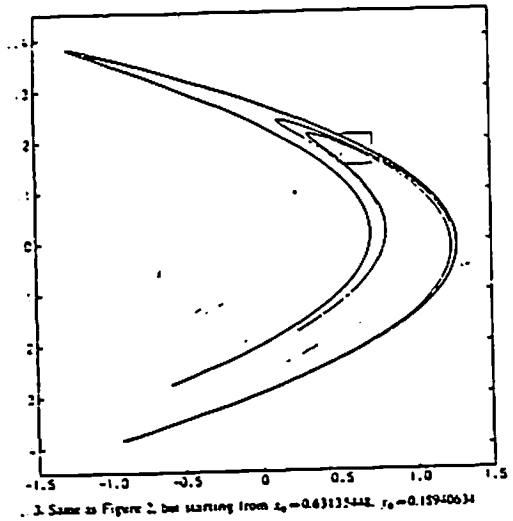

. 3. Same as Figure 2, but starting from $x_0 = 0.63135448$, $y_0 = 0.15940634$

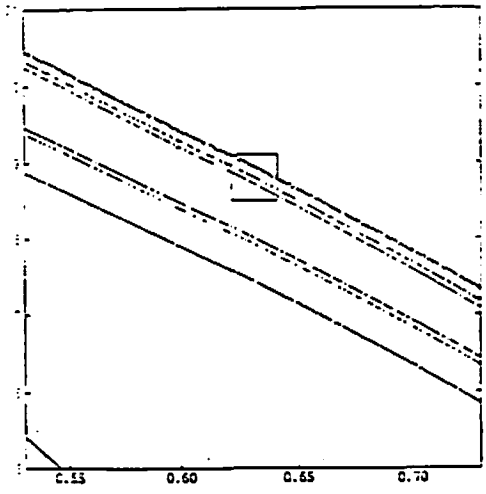

- Enlargement of the squared region of Figure 3. The number of computed points is increased $\times 10^2$

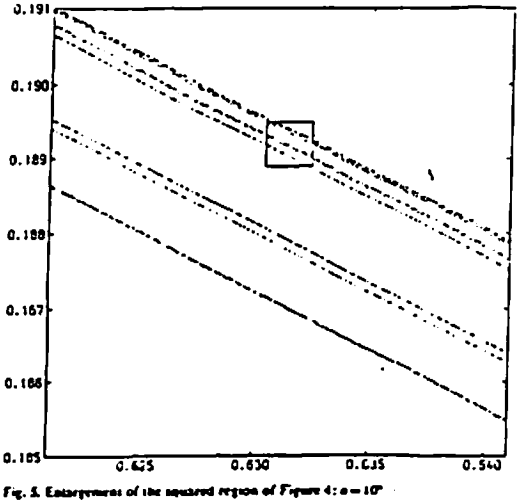

Fig. 5. Enlargement of the squared region of Figure 4: $a = 10^6$

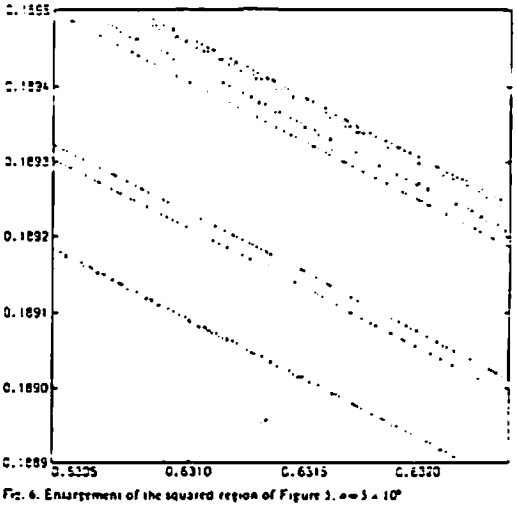

Fig. 6. Enlargement of the squared region of Figure 5. $a = 5 \times 10^6$

There are several routes that a deterministic system can take to chaotic behavior. Perhaps the simplest to examine is what has come to be known as 'the period doubling route to chaos' or 'Feigenbaum's universality'. Central to the study of this phenomenon is the quadratic iterator: x(i+1) = rx(i)*(1-x(i)). What we see is that the same simple, and completely determinate, system governs both orderly and chaotic behavior. As we increase the value of the parameter 'r' from 2 to 4, we can trace a very definite 'route' from order into chaos. That is, when we start with r=2, x(i) for any i large will be one particular point. As we slowly increase r, there is a bifurcation, and our system oscillates between two different values of x(i) for i large. Then, at a certain point each of these values bifurcates, giving us four solutions. This continues on, and we get 2^3, 2^4, 2^5, ... solutions. Feigenbaum discovered that the ratio of the differences in r-values of successive bifurcations is a constant. Please see figure T0. Furthermore, the number δ is a constant regardless of what particular system is exhibiting this period doubling phenomenon. Similarly, the relative scale of the splittings, $\varepsilon_1 / \varepsilon_2$,is constant.

If this were true, if the distances between successive bifurcations was a geometric series, then there is a point to which this series converges. This point would mark the end of the period doubling region. In the logistic map given above, this point is r=3.5699456..., and is referred to as r-infinity. This point divides the final-states diagram into two regions, the period doubling region to the left and the one governed by chaos to the

TO : relative spacing of bifurcation pts and splittings

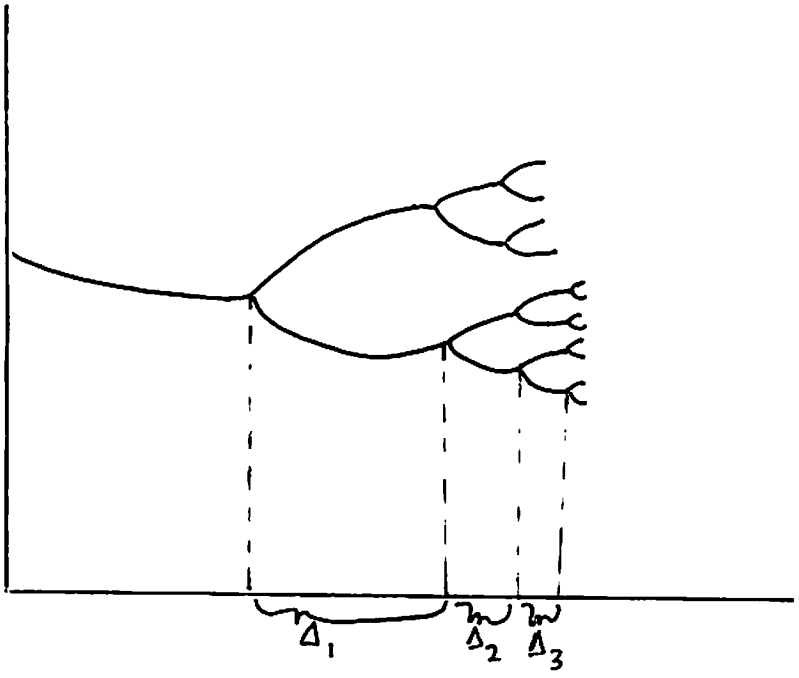

for i large $\Delta i / \Delta_{i+1} = \delta = 4.6992....$

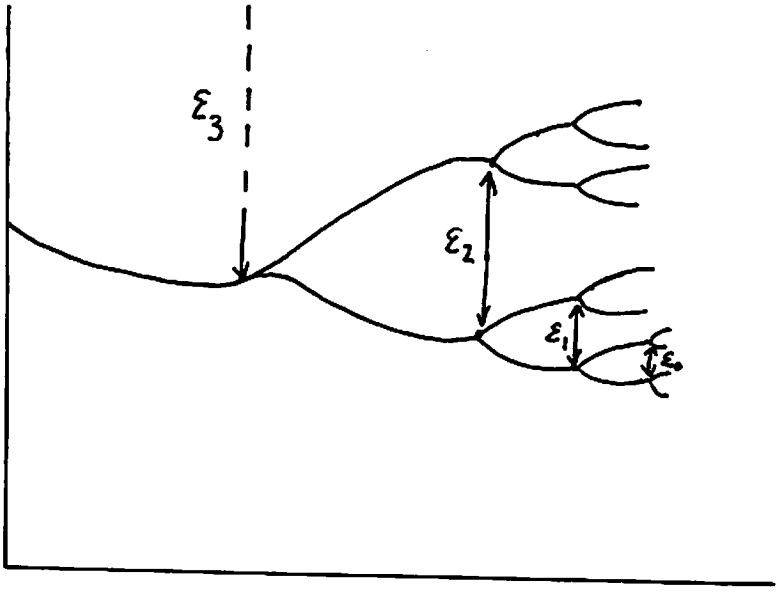

for i small or negative $\varepsilon_{i+1} / \varepsilon_i = \alpha = 2.502....$

right. Please see Figure B1 (after page 9)

However, the right-hand region of the final-states diagram is not merely chaotic, but displays regions of ordered behavior as well. These ordered regions arise in what are called 'periodic windows'. The peculiar self-similarity of these regions is explored in the discussion in the following section.

Surprisingly, the bifurcation diagram, B1, of the mathematical system is topologically equivalent to that of any physical system that follows the 'period doubling route to chaos'. A circuit can be constructed to model the behavior of a generic driven, non-linear oscillator. In fact, with a driving voltage, an inductor, a resistor, and a pn junction with an effective capacitance, we can construct a circuit that <u>is</u> a driven, non-linear oscillator. The effective capacitance of the pn junction used in the circuit sketched below (fig.T2) is roughly $C_o exp(eV/kt)$. When forwardly biased, the junction conducts like a diode, i.e.

$$I_d(V) = I_o exp(ev/kt) - 1$$

The equations that govern the behavior of the circuit are:

$$\dot{I} = [V_o(t) - RI - V] / L$$
$$\dot{V} = [I - I_d(V)] / C(V)$$

With the driving voltage $V_o(t) = V_{oo} sinwt$

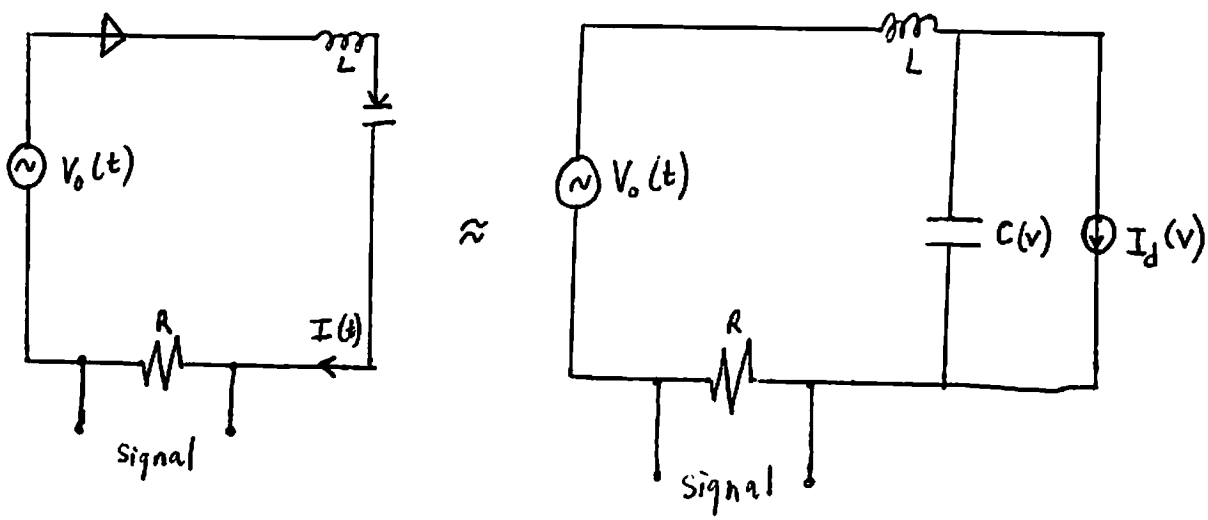

T2: CIRCUIT SKETCH. Non-lin. driven oscillator

What we have is a determinate system that is dissipative and has an easily controllable parameter, V_{oa}. These are the only preconditions of the possibility of getting a physical system to display chaotic behavior. We hope that by gradually increasing V_{oa} we see period doubling all the way to chaos.

Procedure, Data, Analysis:

Before running the actual experiment, I decided to get a feel for the data reduction involved by running a simple simulation. Program osc1 outputs a discrete time series of the function

$$y(i)= (a1)\sin(2\ (f1)ti) + (a2)\sin(2\ (f2)ti) + k(a1)(a2)\sin(2\ (f1)ti)*\sin(2\ (f2)ti).$$

This is just a model of two oscillators and their non-linear cross term. Considering that the real data we'll be taking will be a discrete time series, this seems a logical first model to work with. We'll need to generate Fourier power spectrums, bifurcation diagrams, and return maps towards getting an analysis of the circuit, so we first manipulate the time series of this simulation to generate those types of maps.

To generate the Fourier power spectrum, we use a discrete fast-Fourier transform algorithm outlined in Brigham (please see appendix 3). Some of the problems that arise in using this algorithm are aliasing and leekage. Aliasing occurs because the time series is a set of discrete points sampled from a continuous wave-form. What happens is, if the sampling rate is slower than or equal to half the period of the wave-form, the points sampled give no information as to the frequency of the wave. This can be illustrated by figure P1.

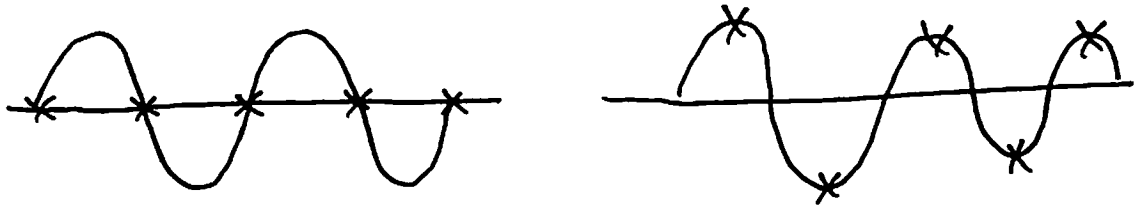

P I : Aliasing at Nyquist Frequency ($\frac{\pi}{2}$)

If the strobe occurs at each 'x' on the wave-form, we can see that when the strobe rate equals half the period of the wave, the two cases shown are equally likely and hence it is impossible to make any interpolation as to the frequency of the wave in question. The computer makes the mistake of thinking there is periodic behavior near the nyquist frequency (T/2). We see four peaks that correspond (left to right) with the non-linear (557 - 330) Hz component, the 330 Hz component, 557 Hz component, and the non-linear component of osc1's output corresponding to (557 + 330) Hz.

Leekage is a consequence of the fact that the time series is a finite truncation of the data series. The sharp transition from a flat base-line to the first data point necessitates the addition of many frequencies to simulate that waveform. Due to this effect, the FFT of a sampled wave is dependant on the phase and frequency of the strobe pulse with respect to the signal. One way to get rid of this problem is to have the series fade in and fade out. That is, attenuate the beginning and end of the series continuously. Fortunately, this was not a measurable problem in our experiment.

We also ran the FFT program using data from a triangle wave generated by a wavetek. We used program P1, to convert the analog signal to a digital time series, then rescaled the data using REDO1 which rescales the data to floating point numbers between zero and one. The Fourier power spectrum plot can be seen in figure P3. As

FAST FOURIER TRANSFORM of OSC1 OUTPUT

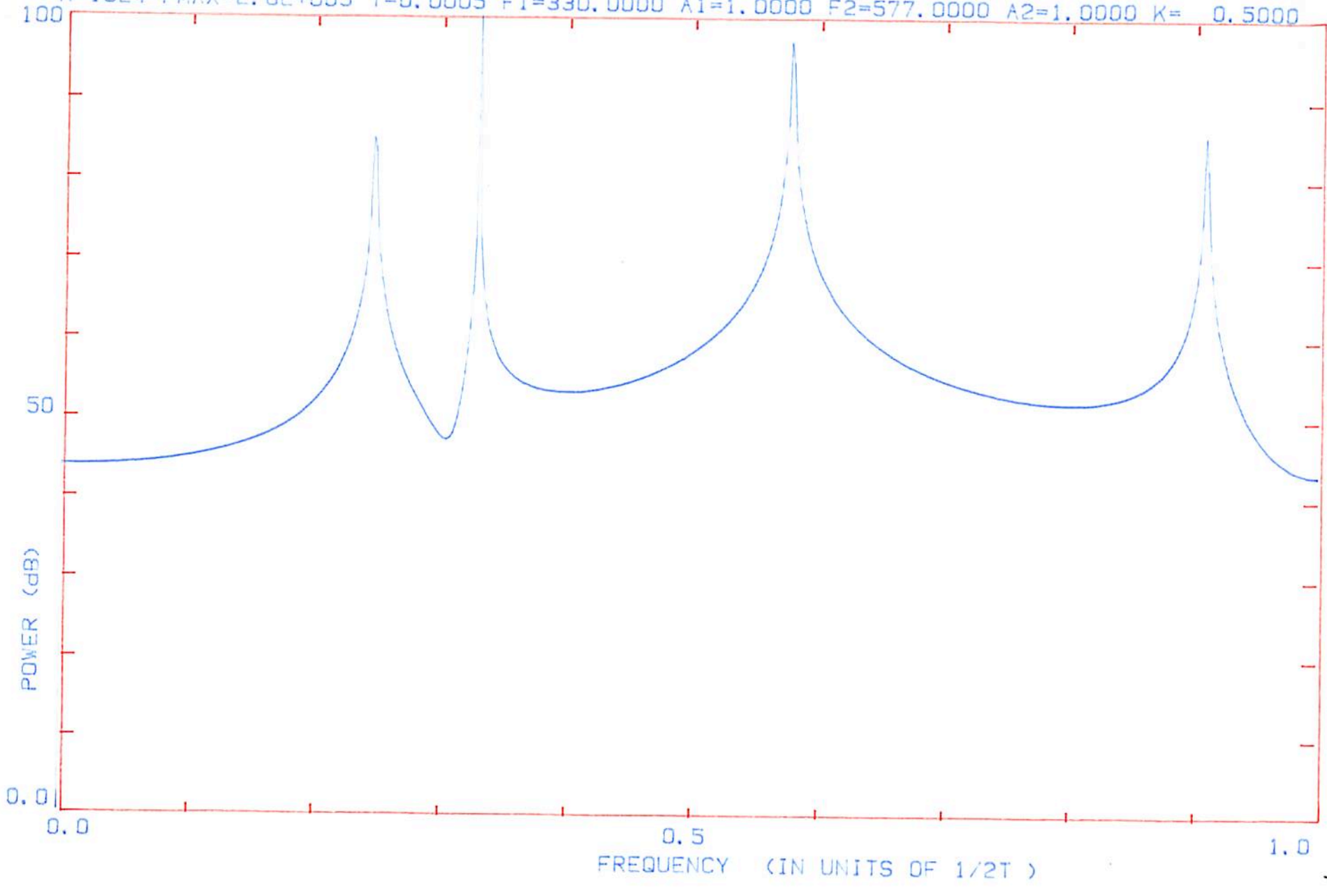

is expected, the spectrum is a series of harmonic peaks of decreasing amplitude.

As has been discussed earlier, the "logistic map" plays a central role in the study of the period doubling route to chaos. We generate the time series by using the simple recurrence relation: $x(i+1) = r*x(i)*(1-x(i))$
Once we've computed the time series, to begin to get a better understanding of what's going on, we plot the return map, bifurcation diagram, and Fourier spectra.

The program used to generate the consecutive iterates throws out the first 1000 iterations to let transients die out. I varied the 'r' parameter and plotted the time series to the screen using as many as 100 iteration points when trying to resolve the higher order bifurcation points. The resolution was such that I could only measure up until the period eight region. Period doubling occurred at r=2.997, period four was achieved at r=3.4485, and period eight at r=3.545. Generating the data via the above recurrence relation on Microsoft Excell, I observed that it is difficult to determine any one point as being the exact bifurcation point. What occurs at the initiation of bifurcation is that for any given parameter value, oscillations around a single solution begin to show up. These oscillations attenuate, but generally very slowly. This behavior is observed in the initiation of bifurcation in the Henon mapping as well. Please see figure H1.

Trying to determine a specific moment of the time series to call the first bifurcation point is hard enough, to try to come up with an accurate measurement for the point where the time series

FAST FOURIER TRANSFORM OF TRIANGLE WAVE (10V p-p)

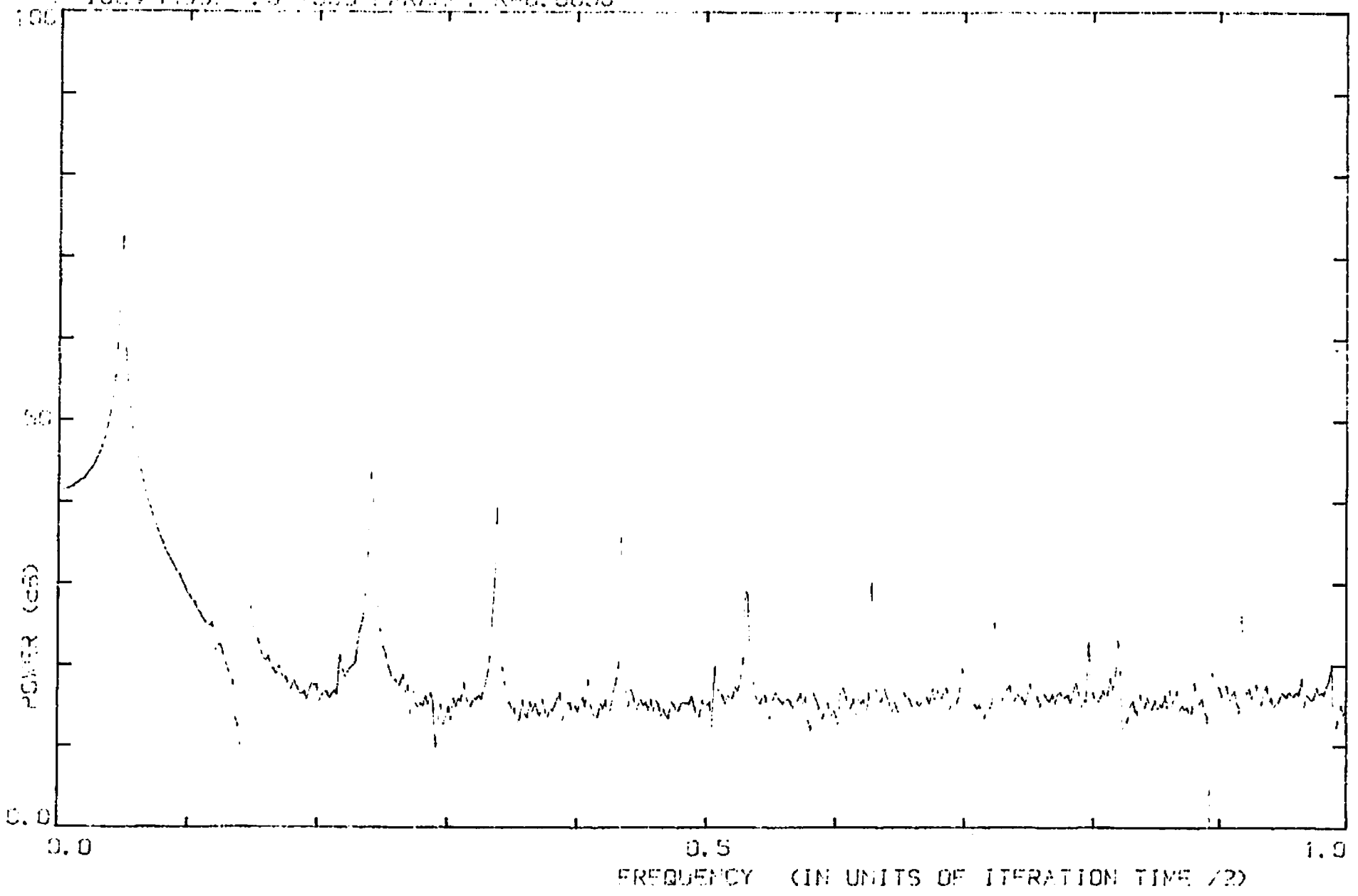

Henon bifurcation diagram

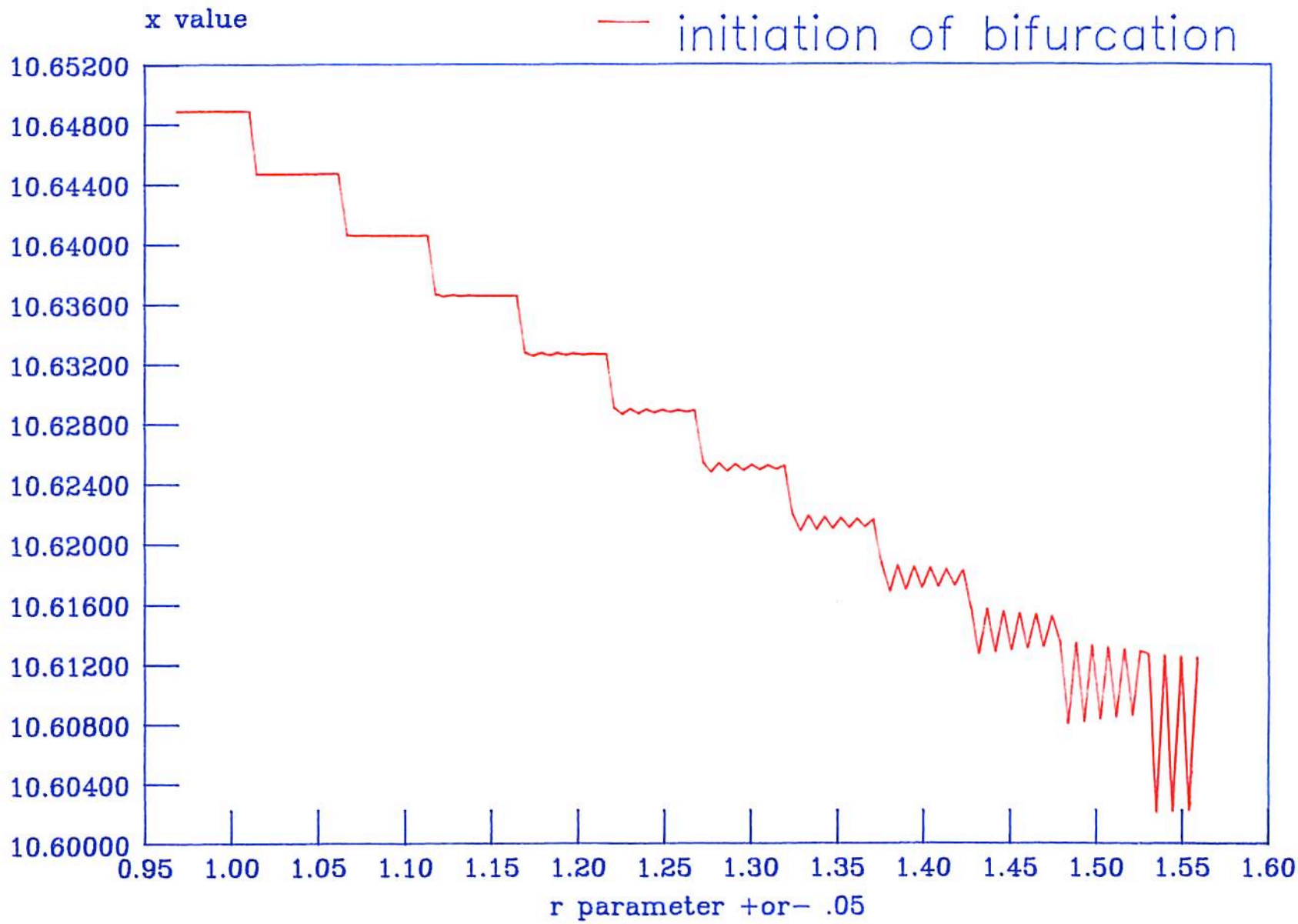

becomes aperiodic we need other methods of representation. To this effect we look at the Fourier spectrum. This too is a judgement call, and at best a fuzzy measurement. Please see figures F1,F2,F3. The three figures correspond to parameters of r=3.5650, r= 3.5700, and r=3.5780 respectively. We'll call the third spectrum (3.5780) the point where the logistic mapping goes aperiodic. Mathematically, this point can be determined rigorously. As Michell Feigenbaum discovered, the ratio of the difference between r-values of successive bifurcations is a universal constant, δ . Thus the series of distances between bifurcation points is geometric. Since the series is convergent, we can determine the limit that the series comes to and this amounts to the point after which the chaotic region begins. r infinity can be determined explicitly given the value for δ . Thus, if δ=4.669201... then r =3.566945....

We get a larger scale view of the situation by plotting several final iterate values of x for each r value between 2.9 and 4.0 . What we generate is the bifurcation diagram, B1. One of the most striking features of the bifurcation diagram are the periodic windows. Starting from the right, we observe a period 3 window, then period 5, then 7, then 9, and so on. Interestingly, the ratio of the differences in r-values of successive windows is the Feigenbaum number, δ ! This mirror-image self similarity brings up some interesting questions. First of all, looking at the period three window, we see that each of the three solutions themselves rapidly evolve through the same bifurcation pattern and have their own r-infinity's. This self similarity leads to the question of

FAST FOURIER TRANSFORM OF LOGISTIC MAP TIME SERIES

N= 512 PMAX=1.1E+006 PARAMETER=3.5650

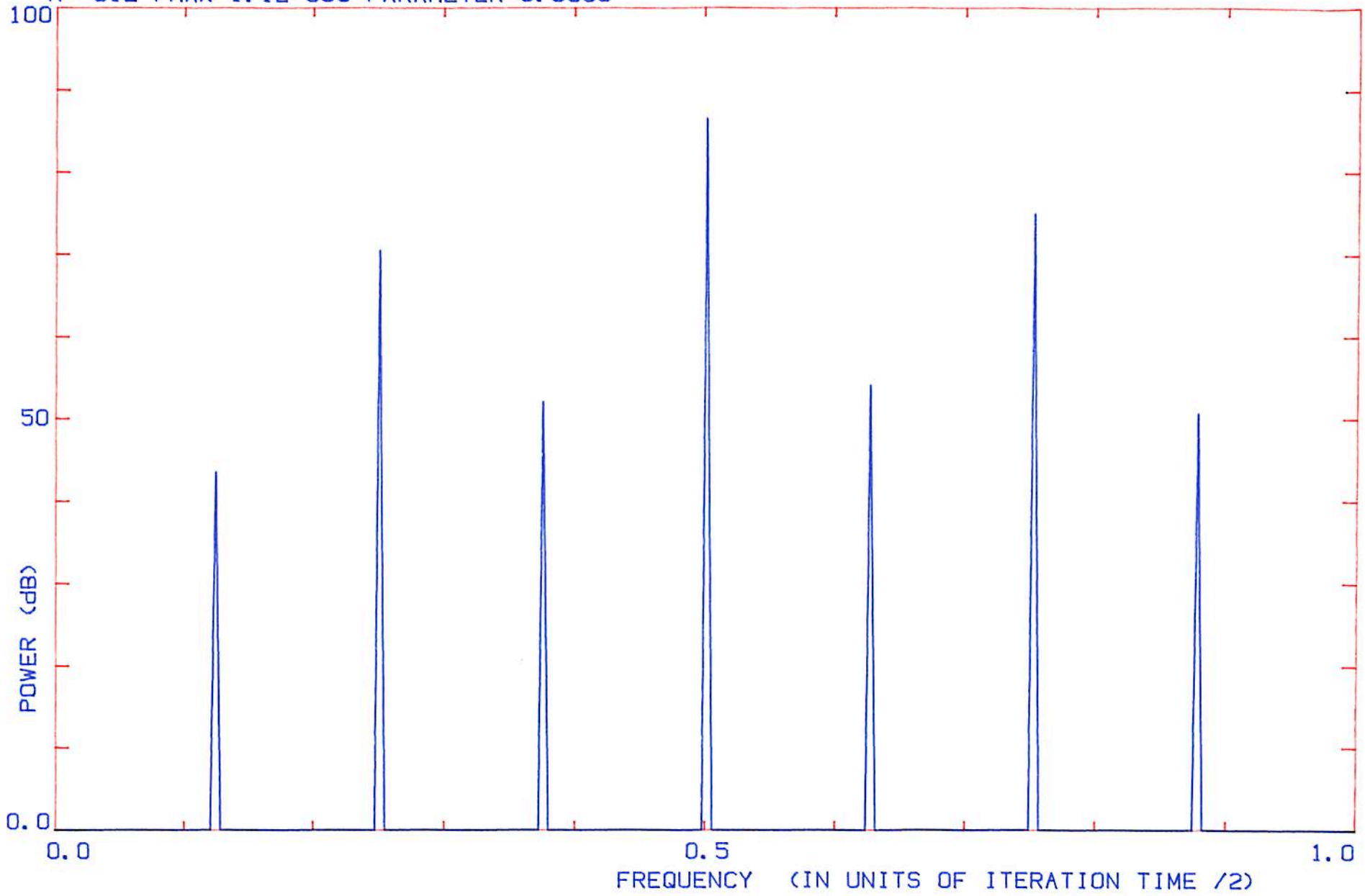

FAST FOURIER TRANSFORM OF LOGISTIC MAP TIMESERIES

N= 512 PMAX=1.1E+006 PARAMETER=3.5700
R

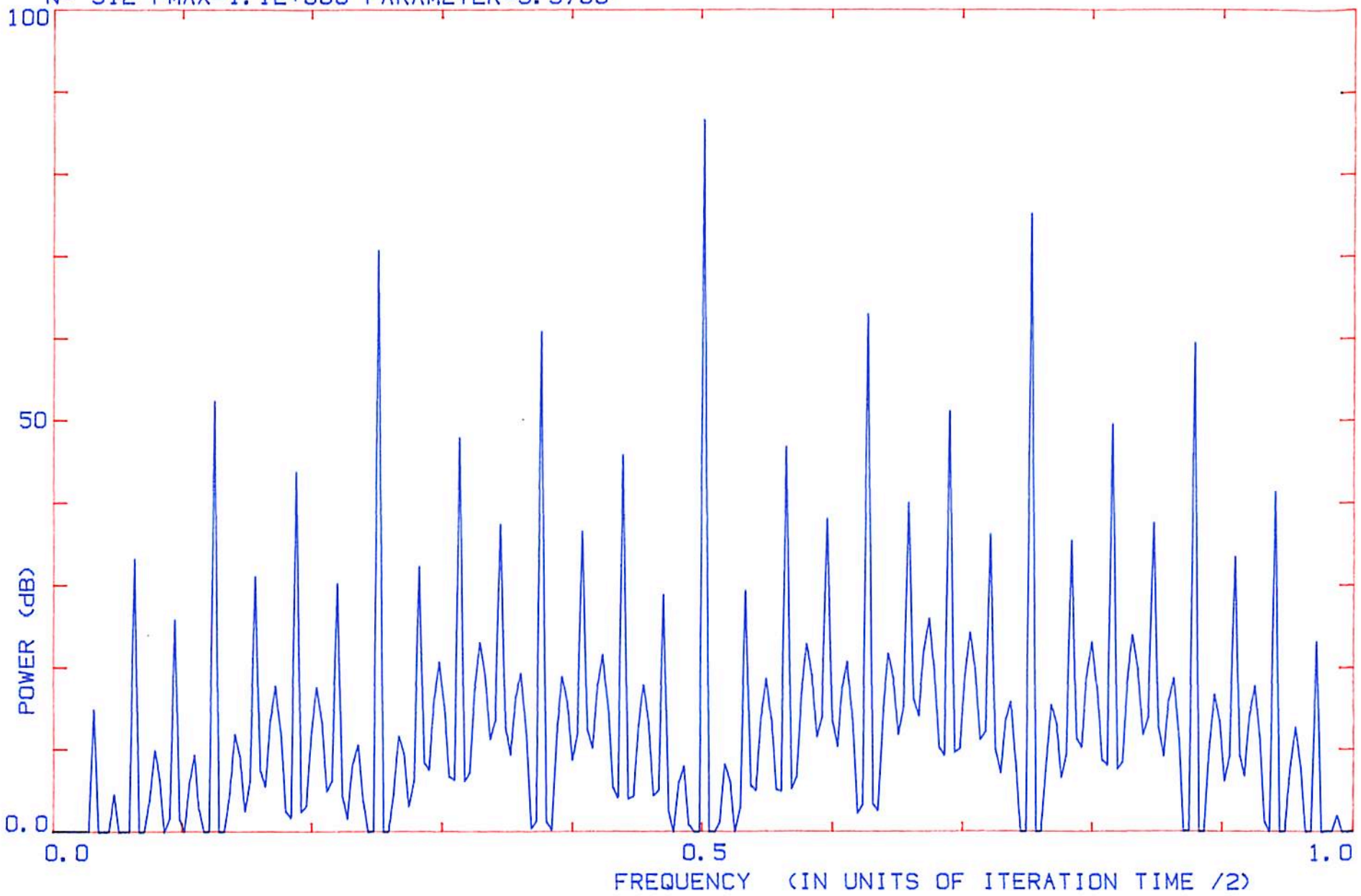

F3

FAST FOURIER TRANSFORM OF LOGISTIC MAP TIME SERIES

N= 512 PMAX=1.1E+006 R PARAMETER=3.5780

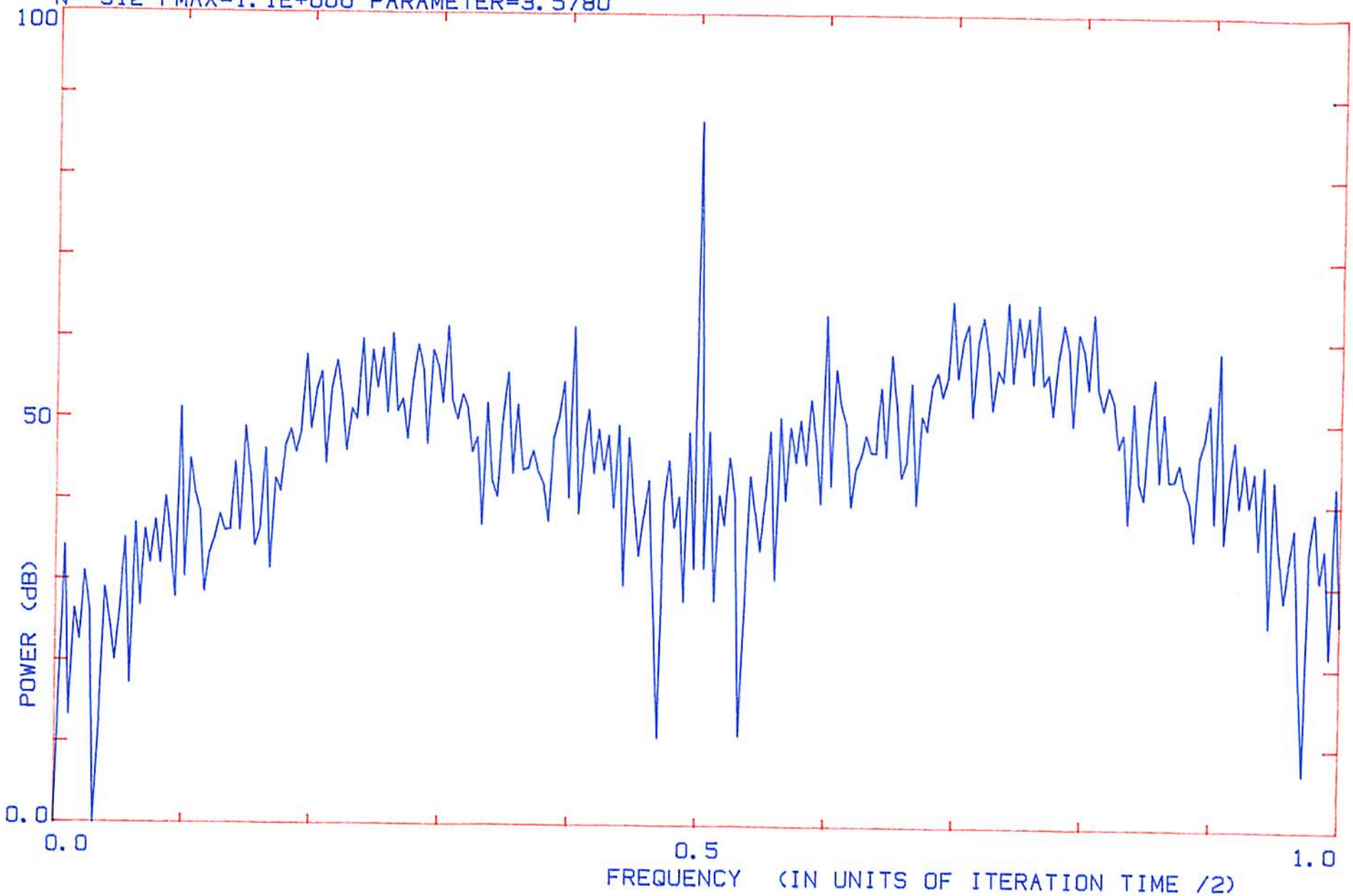

F3

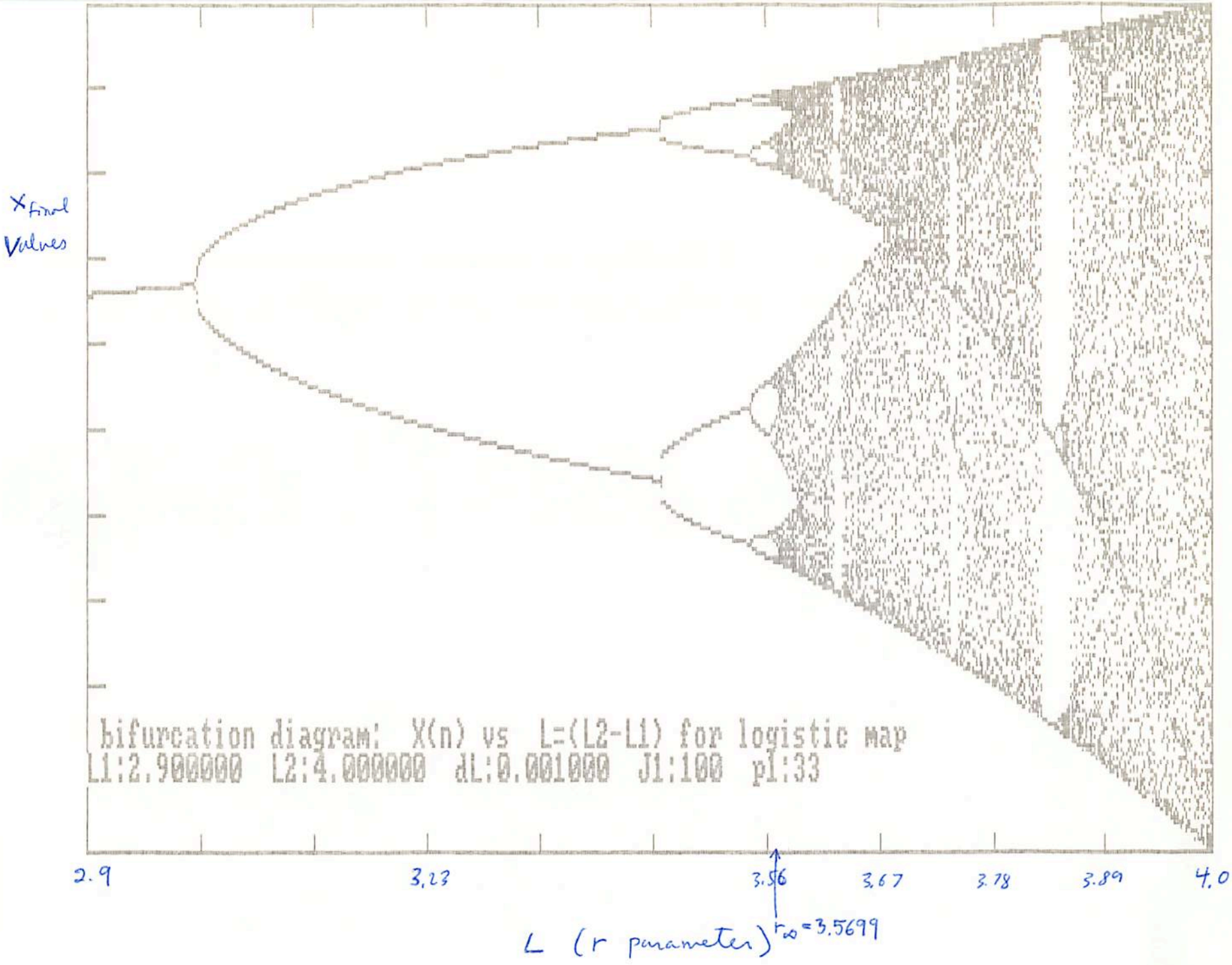
X_{final} Values
bifurcation diagram: X(n) vs L=(L2-L1) for logistic map
L1:2.900000 L2:4.000000 dL:0.001000 J1:100 p1:33
2.9
3.23
3.56
3.67
3.78
3.89
4.0
L (r parameter)
$r_\infty = 3.5699$

rapidly evolve through the same bifurcation pattern and have their own r-infinity's. This self similarity leads to the question of whether we can trace the splitting back past the beginning of our bifurcation diagram. Are there other aspects at the beginning of the iteration that we were unaware of? Is our bifurcation tree just one branch of a larger tree? If this is so then there is really no beginning to the bifurcation diagram, and it would never make sense to speak of any particular r-infinity since each branch has its own r-infinity. The measurement of r-infinity would be relative to a particular reference frame, and it is even possible that (if there is indeed no limit as to how far the splitting can be projected back) for any value of r, we can find a branch in reference to which it is an r-infinity.

At first look, there seems to be no reason why our initial condition must be x(0)=0. Consequently, we should be able to see a second solution around a larger x-value for a parameter value of $r < 3$. Since the vertical spacing between successive splits on the bifurcation diagram follows the same type of universality law that gives the Feigenbaum ratio (See figure T0). If we know what ε_1 and ε_2 are, we can calculate ε_3 and predict an x(0) that will give us a period two solution for r just less than 3. Using an initial x-value of .1, from the data generated by Excell, I determined the ratio $\varepsilon_2/\varepsilon_1 = 2.502$, with $\varepsilon_2 = .41$. From this we can determine $\varepsilon_3 = 1.0258$. Adding this to the original initial condition, we get 1.1258. However, when we use this number as a new initial condition by plugging into the recurrence relation, the relation quickly diverges. In fact, for any x-value over 1, the

series diverges. So we see, there is a limit to how far back we can trace the splitting. There is a rightful beginning to our bifurcation diagram because the "logistic map" only converges as a mapping of the unit interval onto itself.

Ok, so with this foray into the world of simulacra behind us, we are now ready to start dealing with the "real" world. What we did was use a pn junction to form a resonator circuit, and ran the Voltage trace to the x-axis and the current trace to the y-axis of a TEK 531A oscilliscope. As we increased the amplitude of the sinusoidal driving voltage incident on the circuit, we indeed observed the period doubling route to chaos.

At V=0.395 + .002 we observed the first bifurcation. The bifurcation threshold measurements had to be taken while only <u>increasing</u> the voltage to avoid error caused by hysteresis. These measurements are displayed in table C1.

V2 = 0.395 + .002 Volts
V4 = 1.244 + .004 Volts
V8 = 1.575 + .016 Volts
V12= 1.665 + .02 Volts (intermittency is observed)
V16 not seen
V5 window = 2.770 to 2.804 Volts
V3 window = 4.666 to 5.222 Volts (doubles at 5.222)

Table C1:Bif.Treshhold data

From this data we can get an estimate of the Feigenbaum number, δ . Using the four measurements made and the formula:

$D = (V_n - V_{n-1})/ (V_{n+1} + V_n)$ gives us two estimates, 2.56 and 3.677. The second of these numbers is less than .21 % off from the accepted value cited above!

After these analog measurements, we took data using an Analog to digital converter using a strobe frequency of 12000 Hz. Again

We plotted the return maps of the circuit for the period four region (figure R1), the chaotic region (figure R2), and the period three window (figure R3). As we see the phase portrait makes four loops before repeating in fig.R1, three loops in fig.R3, and doesn't seem to join itself at all in fig.R2.

We also plotted the Fourier spectra of data taken from the period 8 region, to compare with the spectra taken from the chaotic region. In figure FT1 we see eight distinct peaks of the period eight region. In figure FT2 we see what amounts to a continuous spectrum of frequencies that corresponds to chaotic behavior.

Next we ran a program called NEWGBD which takes 300 steps, gathering 16 data points at each step from V incident on the circuit equal to .03 Volts to V = 4.5 Volts. We then plotted this data in the bifurcation diagram of figure B2. Though the resolution (16 points per parameter value) is poor in the chaotic regions, we can see the remarkable similarity with the bifurcation diagram generated by the logistic map. Furthermore, the beginning of a self-similar region can be observed quite clearly at the top middle of the diagram.

In general, it's remarkable how clearly this circuit exhibits the period doubling route to chaos. The similarity between the physical system and the theoretical "logistic map" model is a strong statement as to the physical applicability of chaos theory.

Next, I decided to look at the Henon mapping. In response to Lorentz' investigation of his famous three first-order differential equations, Henon showed that the same properties can be observed

Return map - period 4 region

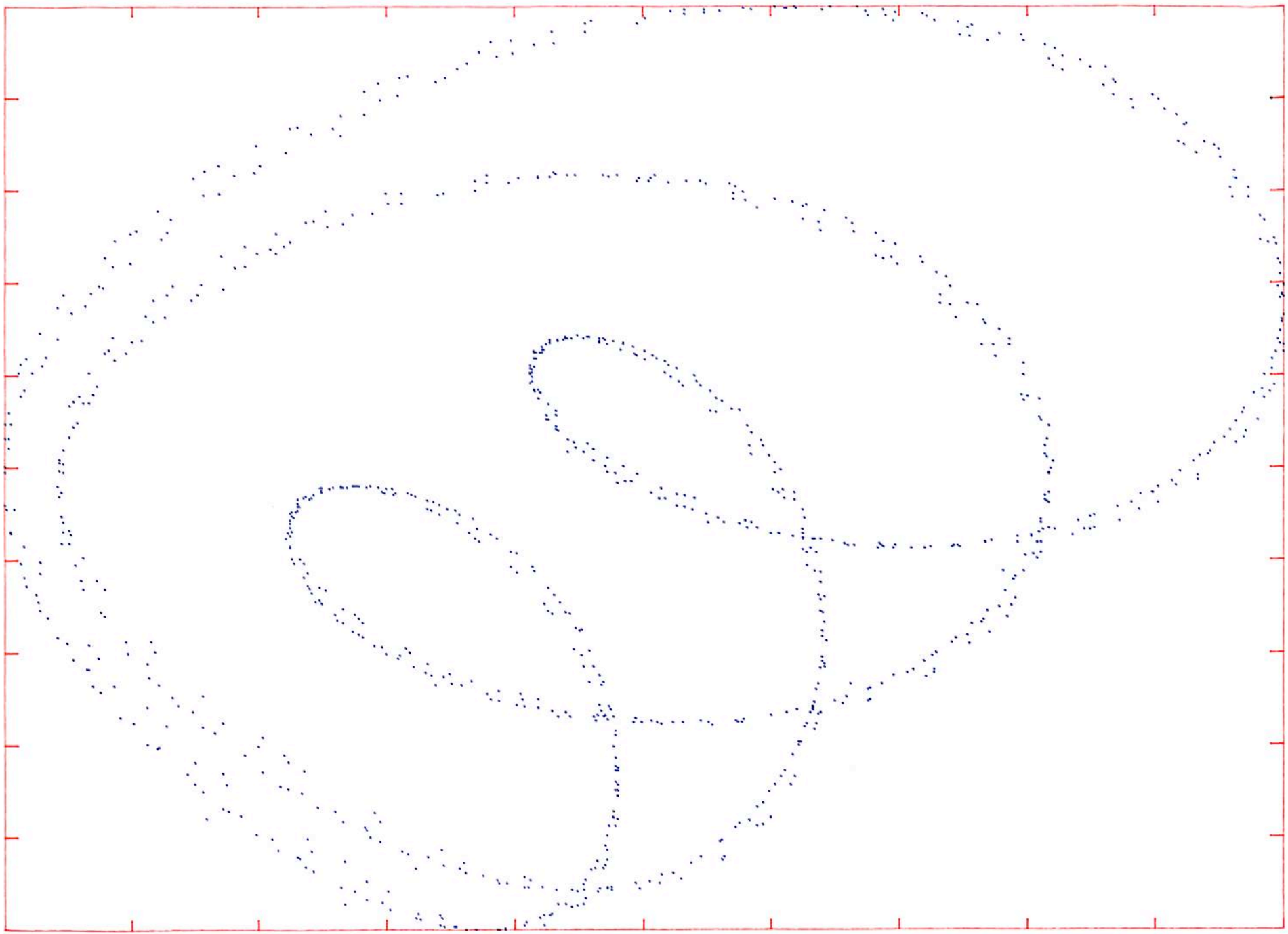

R4

Return map- chaotic region

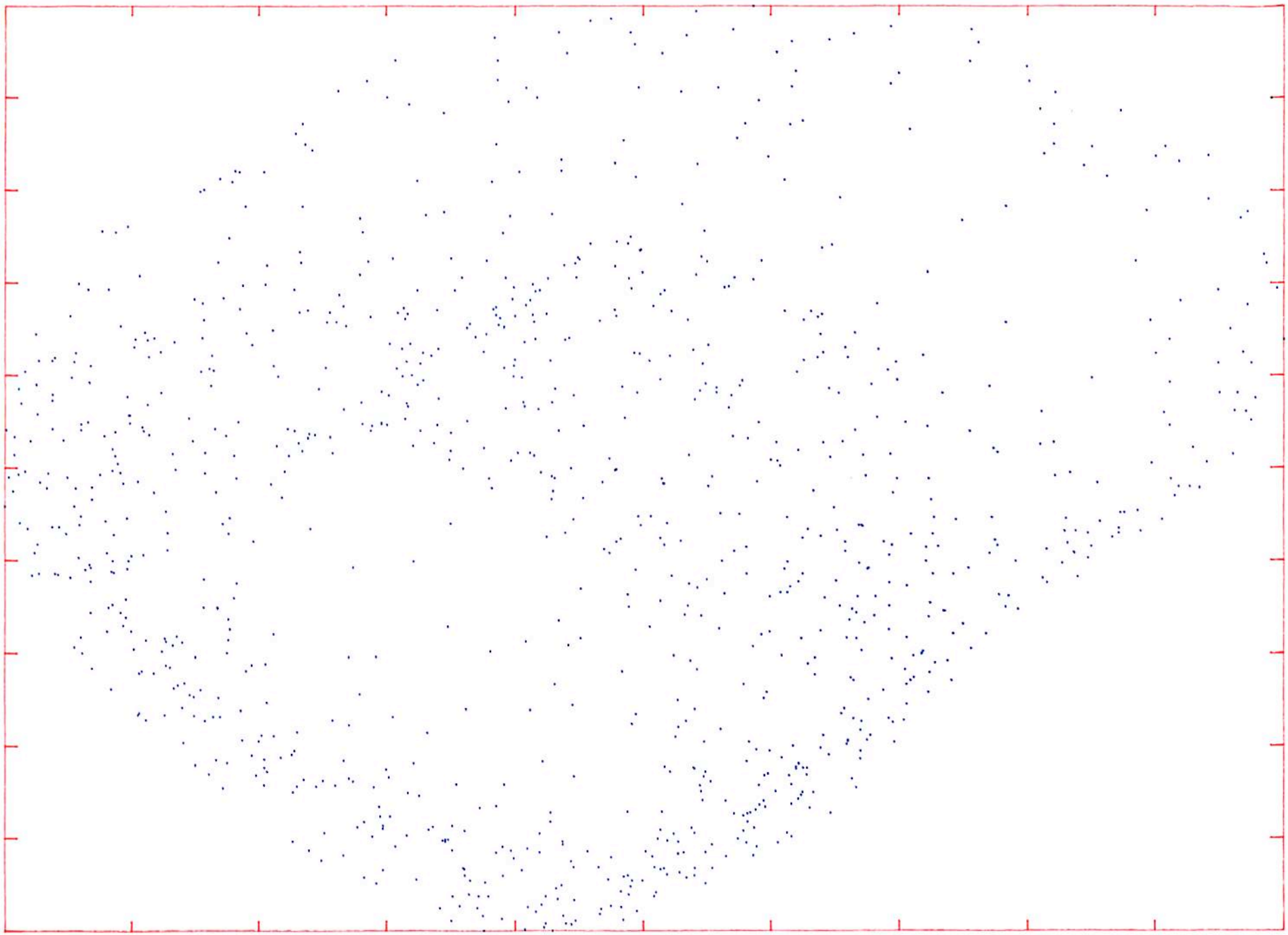

R2

Return map – period 3 window

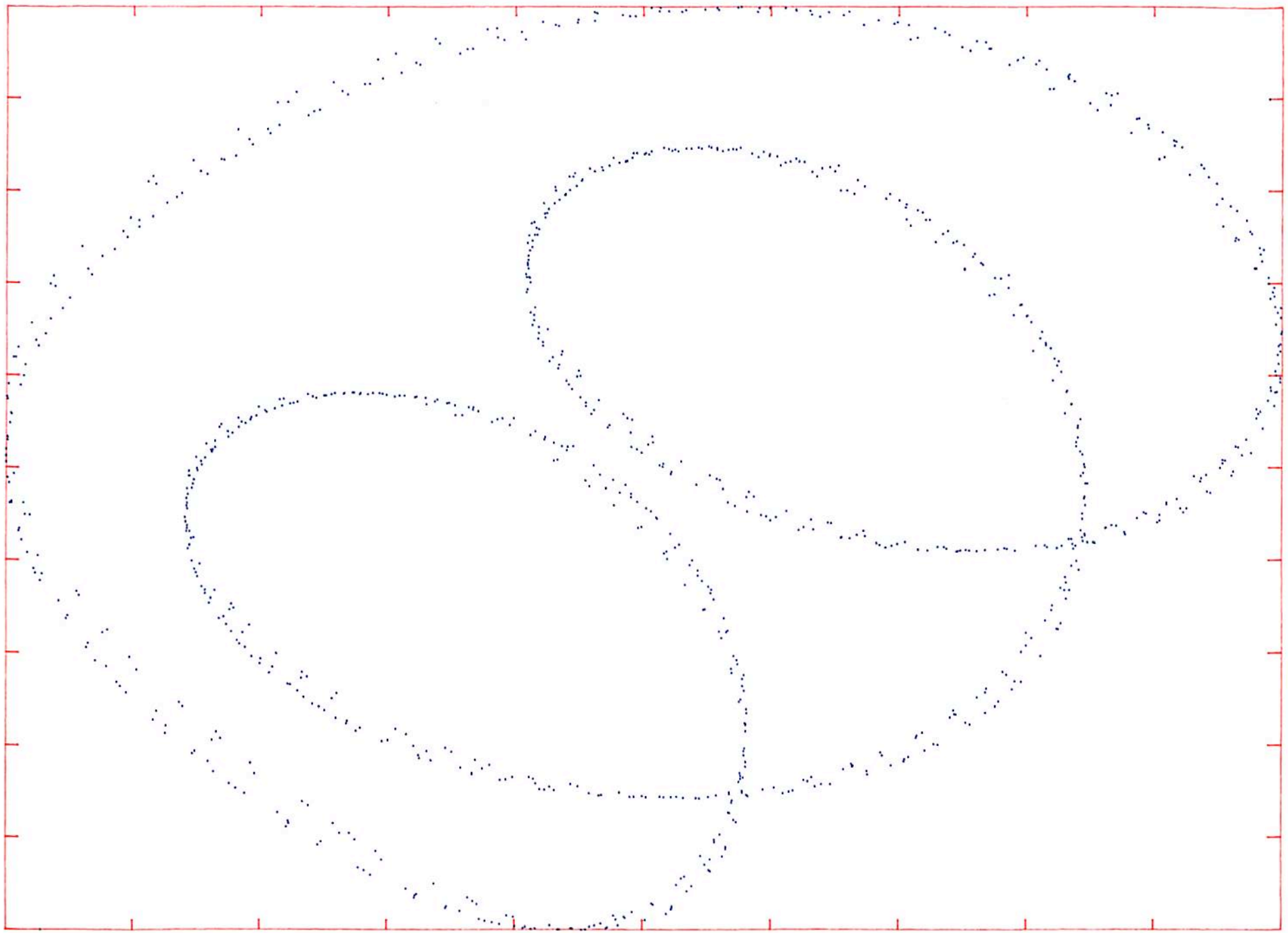

Spectrum of Fourier Transform Period 8 Region in Circuit expt

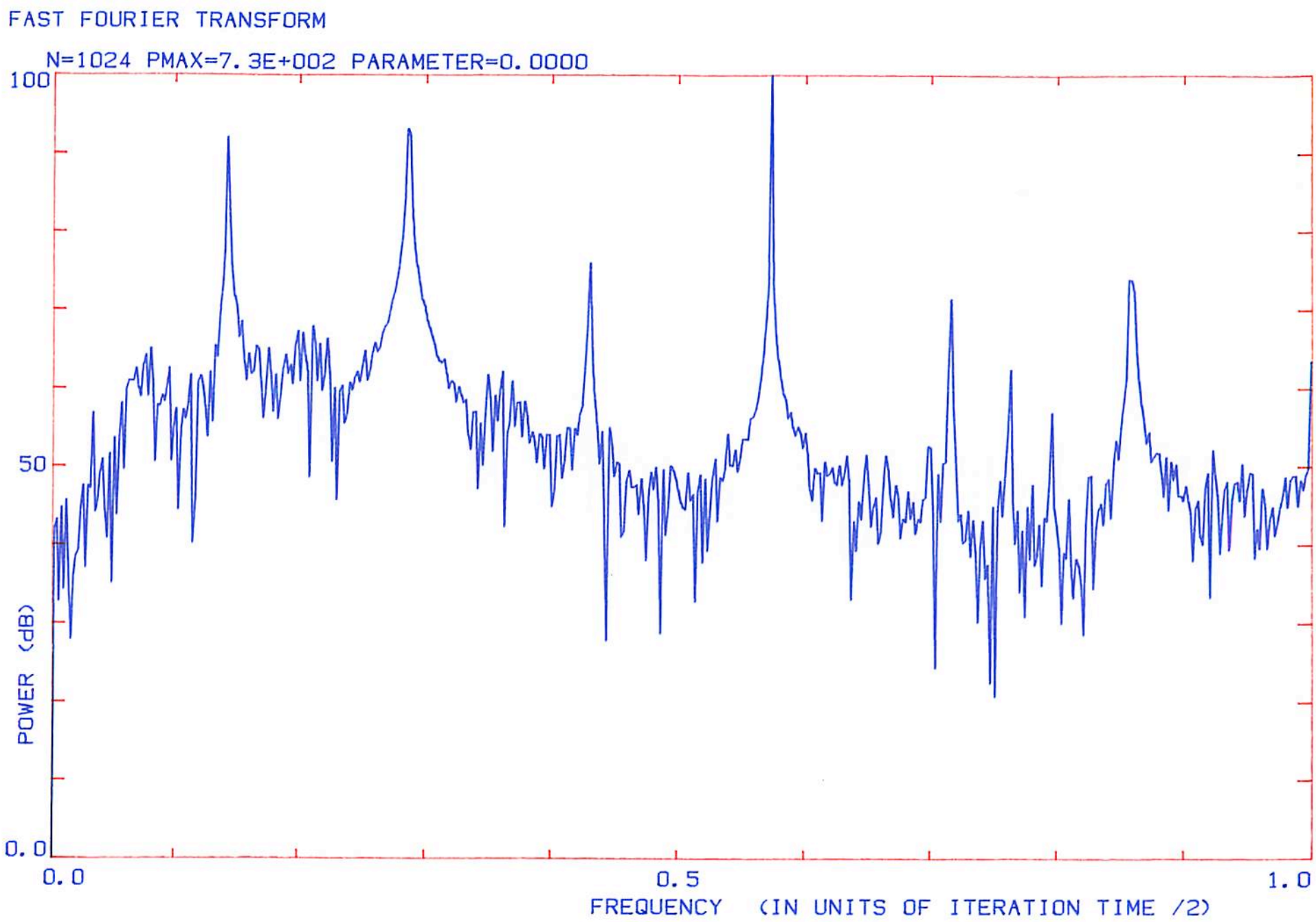

FT1

Fourier Spectrum chaotic region in Circuit expt.

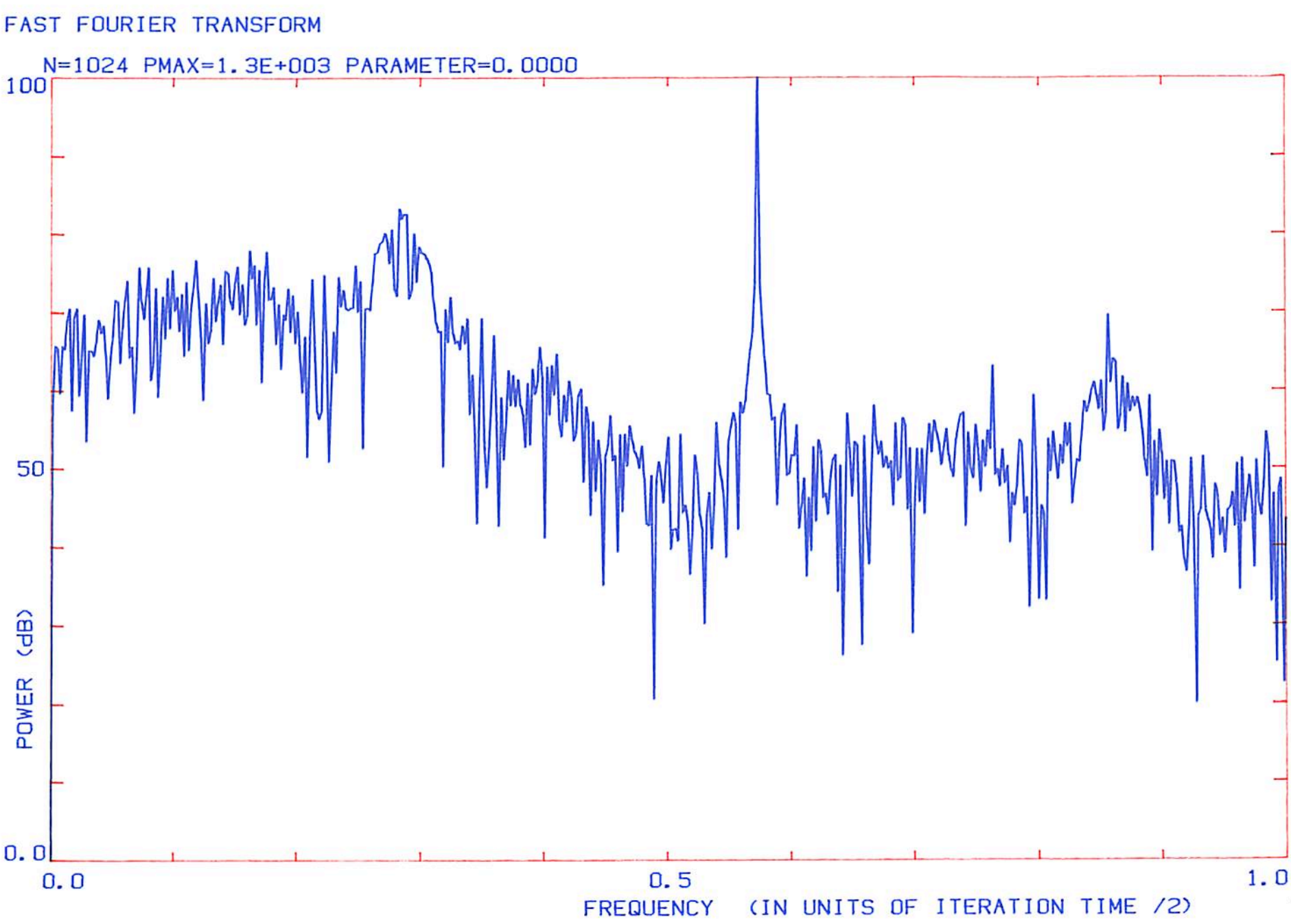

FT2

FT2

Bifurcation Diagram Circuit Experiment

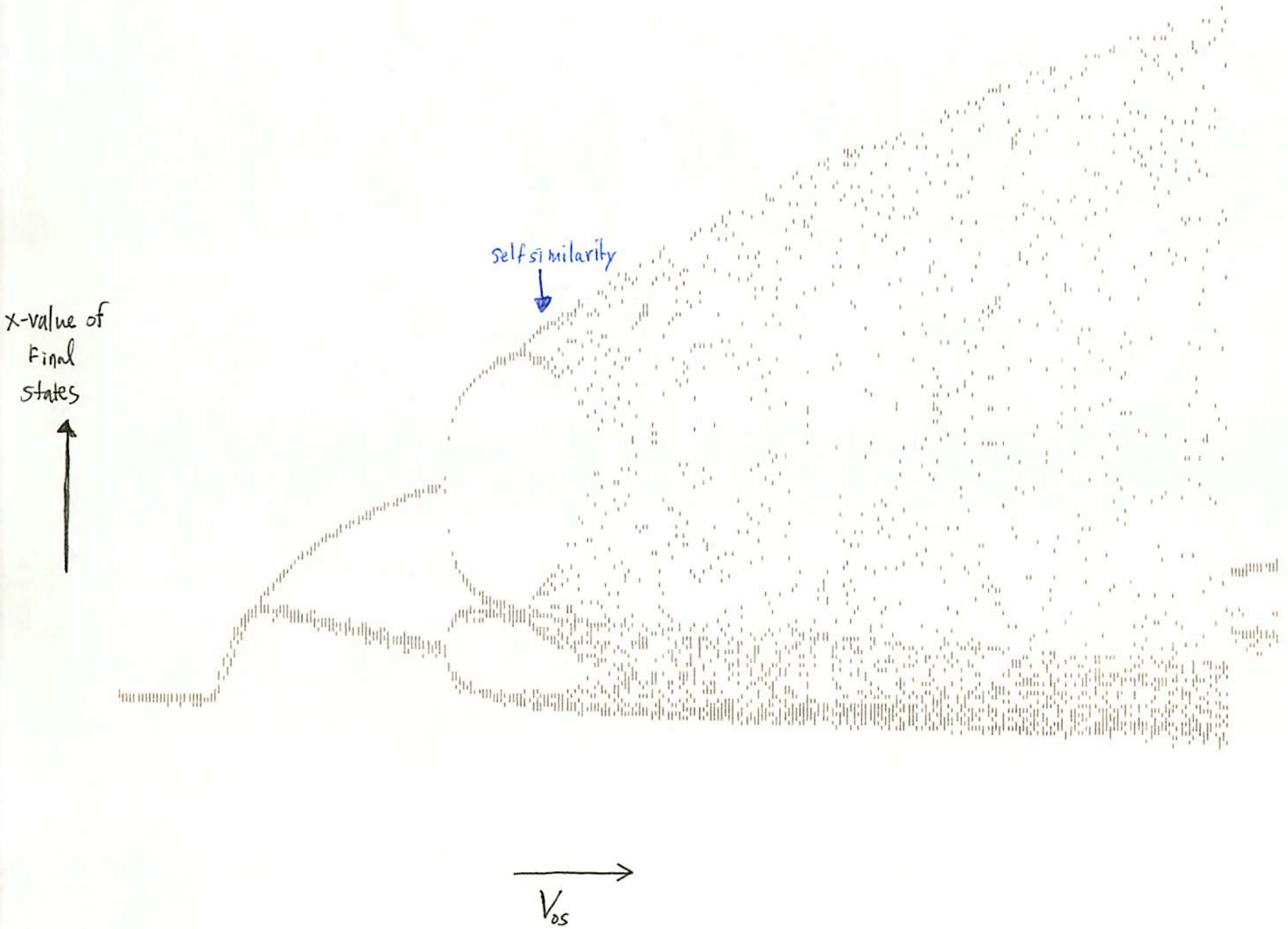

mapping. In response to Lorentz' investigation of his famous three first-order differential equations, Henon showed that the same properties can be observed in a simple mapping of the plane defined by the recurrence relation: $x(i+1) = y(i) + 1 - qx^2(i)$, $y(i+1) = px(i)$. What Henon did was look at the Poincaré map of a trajectory as a mapping of the plane to itself. By seeing that "the essential properties of the trajectory are reflected into corresponding properties of the set of points", Henon reduced the problem to the study of a two-dimensional mapping.

I split my inquiry into two parts. The first I did on Microsoft Excell, the second using my own Fortran program and Analyze for the IBM. My objective in the first part was to graphically represent the behavior of the mapping as I increased the parameter value, q. On Excell, I generated the time series of the mapping using the recurrence relation mentioned above. And then plotted the return maps of the generated serieses using Excell's plotting options. I varied q from .5 to 1.8 using the same initial conditions each time. This is represented in the series of eight graphs attached ('henon 1-8'). We see that the return map rapidly evolves to a strange attractor. This attractor can be shown to be chaotic by demonstrating sensitivity to initial conditions in the behavior of the time series.

To this effect, I did a series of runs keeping the q and p parameters fixed, but shifting the initial condition of the system. These runs are represented in the four graphs, 'sic 1-4'. The first graph has initial condition (x,y) = (0,0). Sensitivity in the form of the return map to initial conditions is apparent.

Henon 1

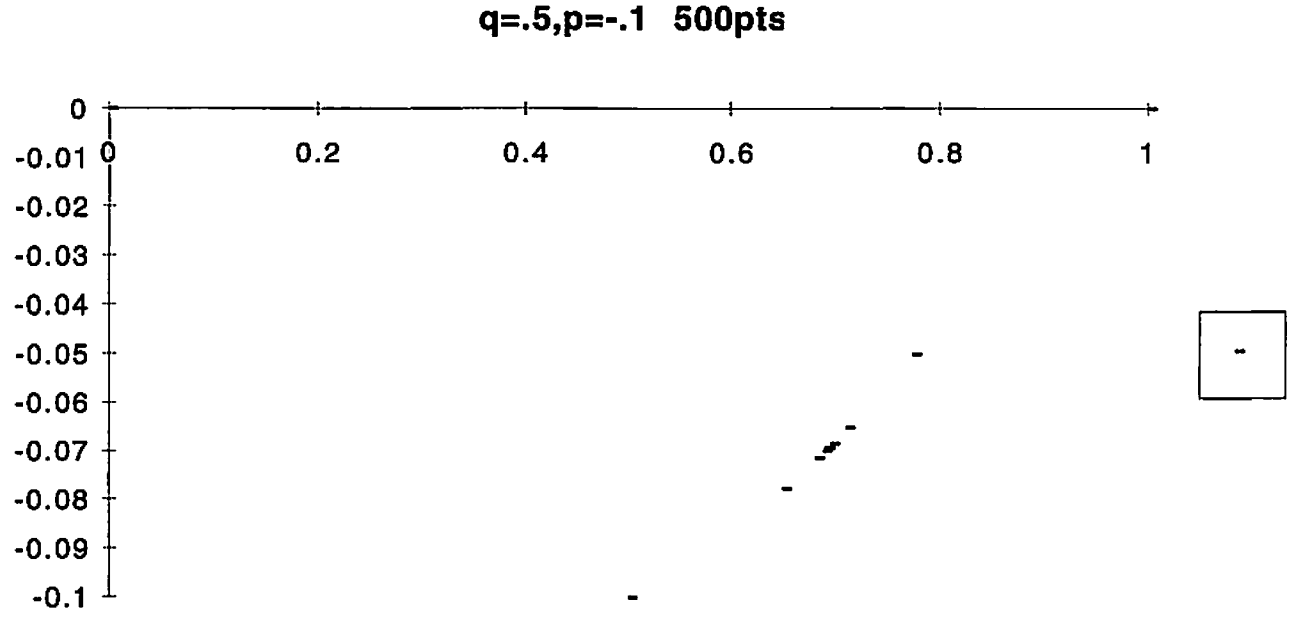
q=.5,p=-.1 500pts
0
-0.01
-0.02
-0.03
-0.04
-0.05
-0.06
-0.07
-0.08
-0.09
-0.1
0
0.2
0.4
0.6
0.8
1

Henon 2

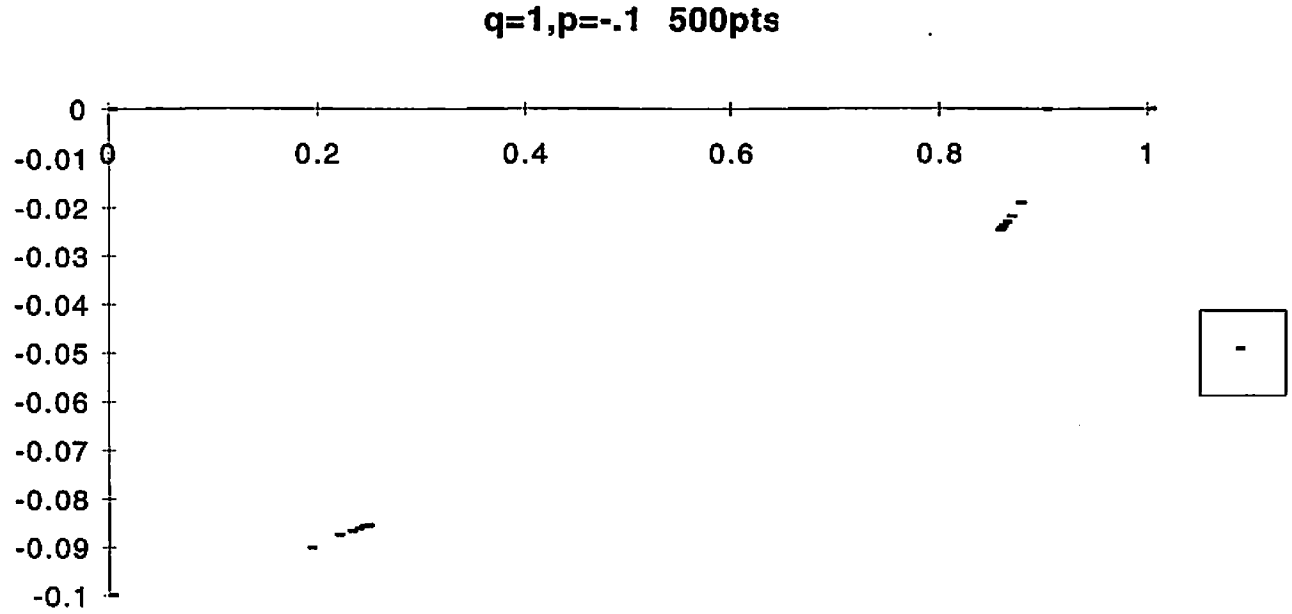
q=1,p=-.1 500pts
0
-0.01
-0.02
-0.03
-0.04
-0.05
-0.06
-0.07
-0.08
-0.09
-0.1
0
0.2
0.4
0.6
0.8
1

Henon 3

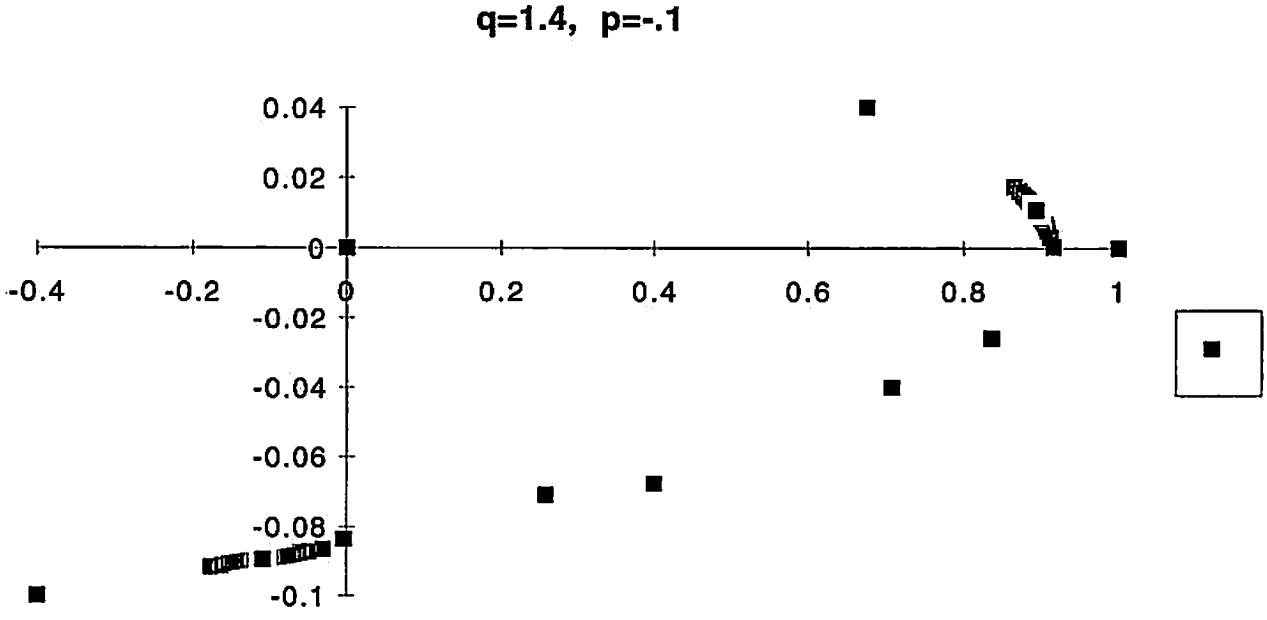

Henon 4

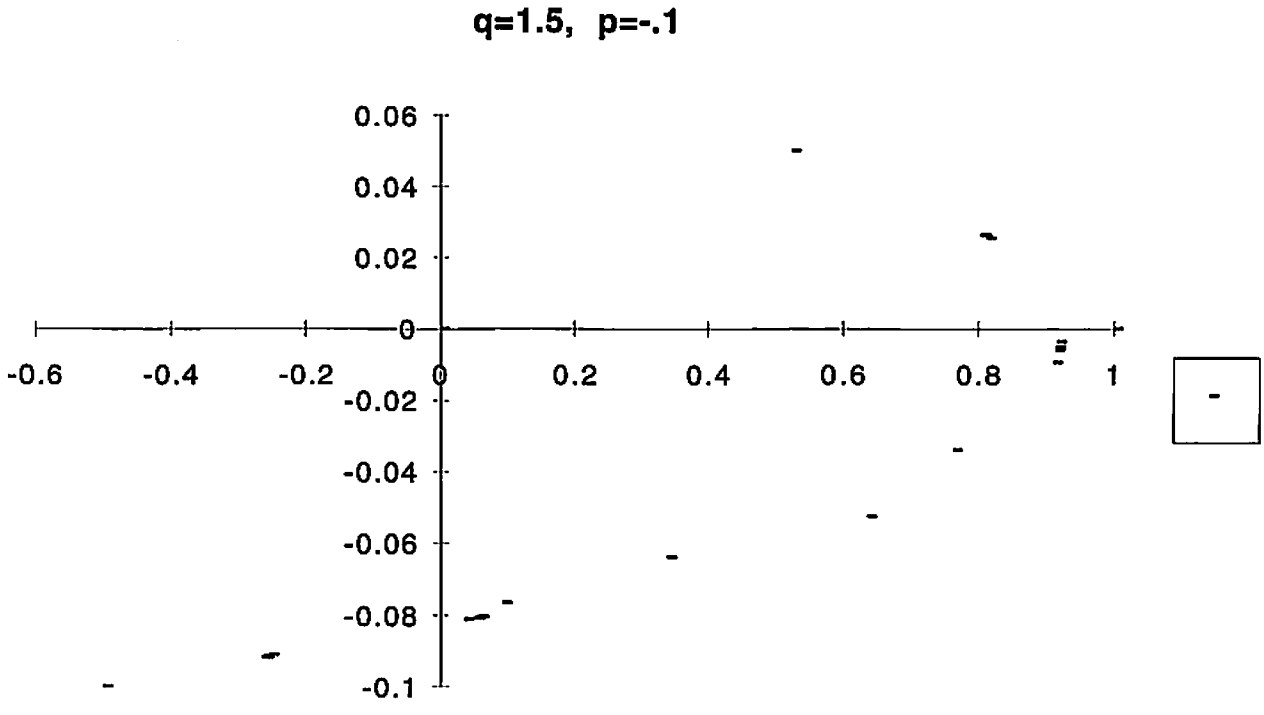

Henon 5

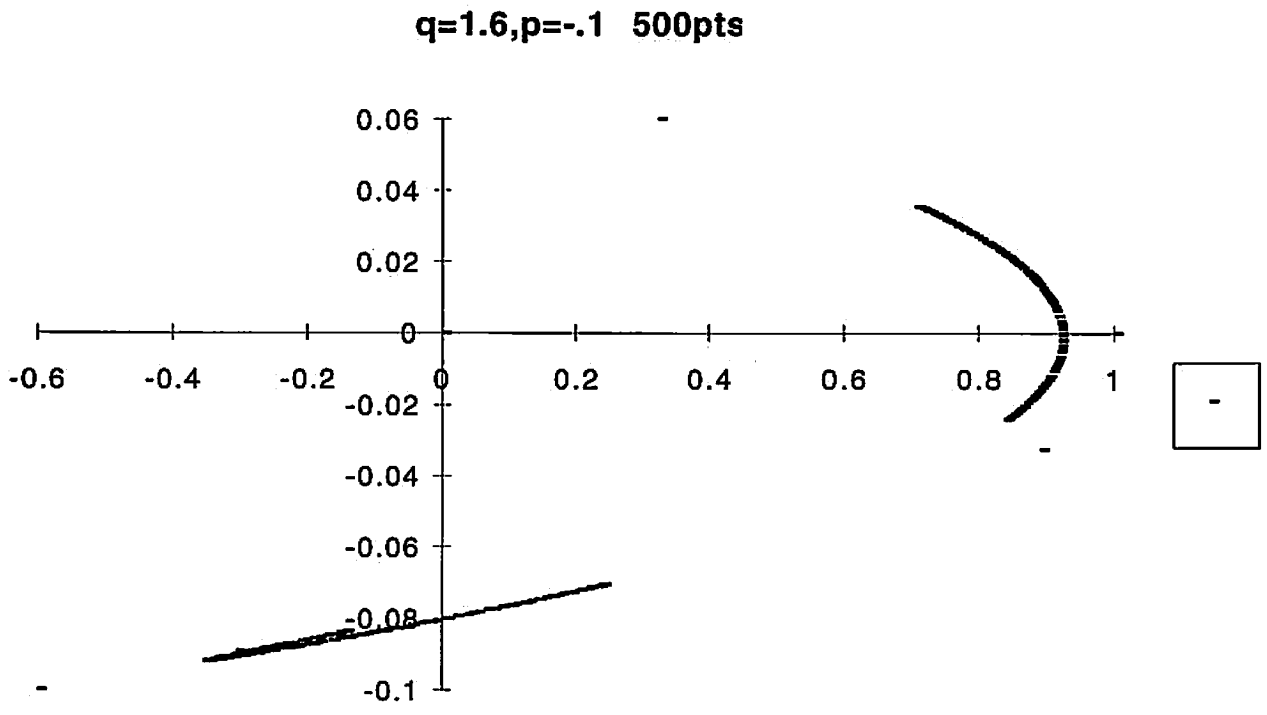
q=1.6,p=-.1 500pts
0.06
0.04
0.02
0
-0.02
-0.04
-0.06
-0.08
-0.1
-0.6
-0.4
-0.2
0
0.2
0.4
0.6
0.8
1

Henon 6

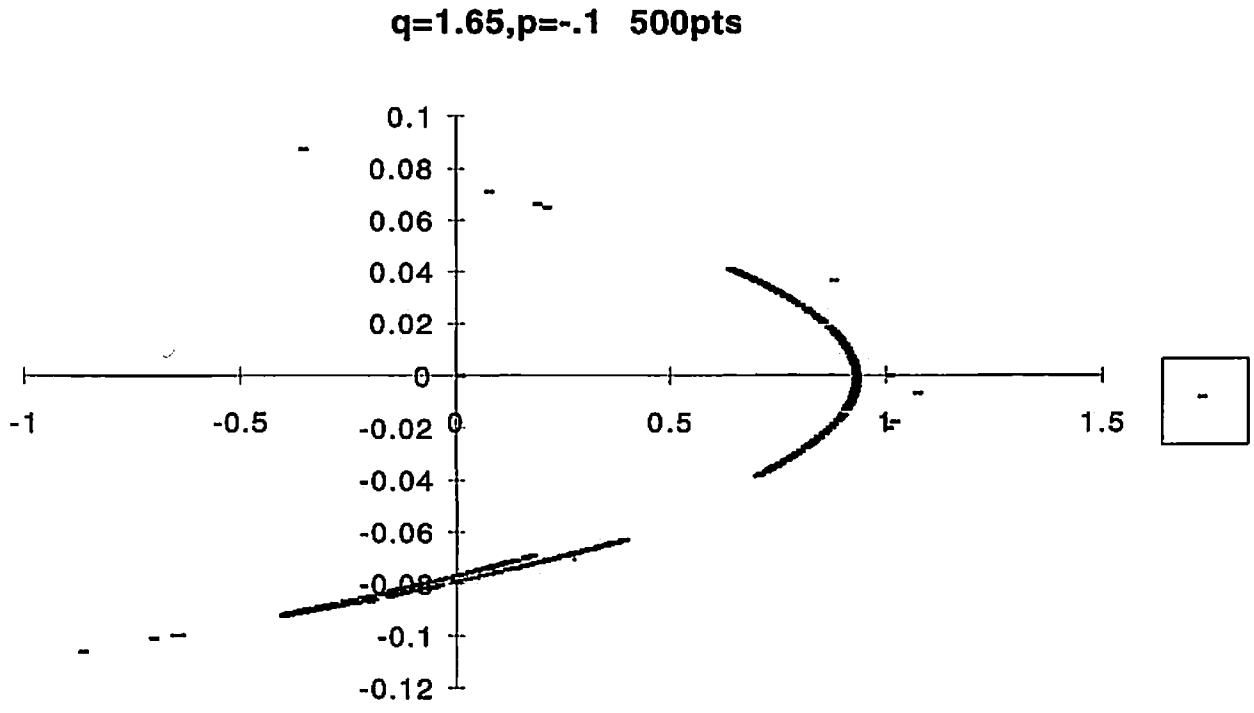
q=1.65,p=-.1 500pts
0.1
0.08
0.06
0.04
0.02
0
-0.02
-0.04
-0.06
-0.08
-0.1
-0.12
-1
-0.5
0
0.5
1
1.5

Henon 7

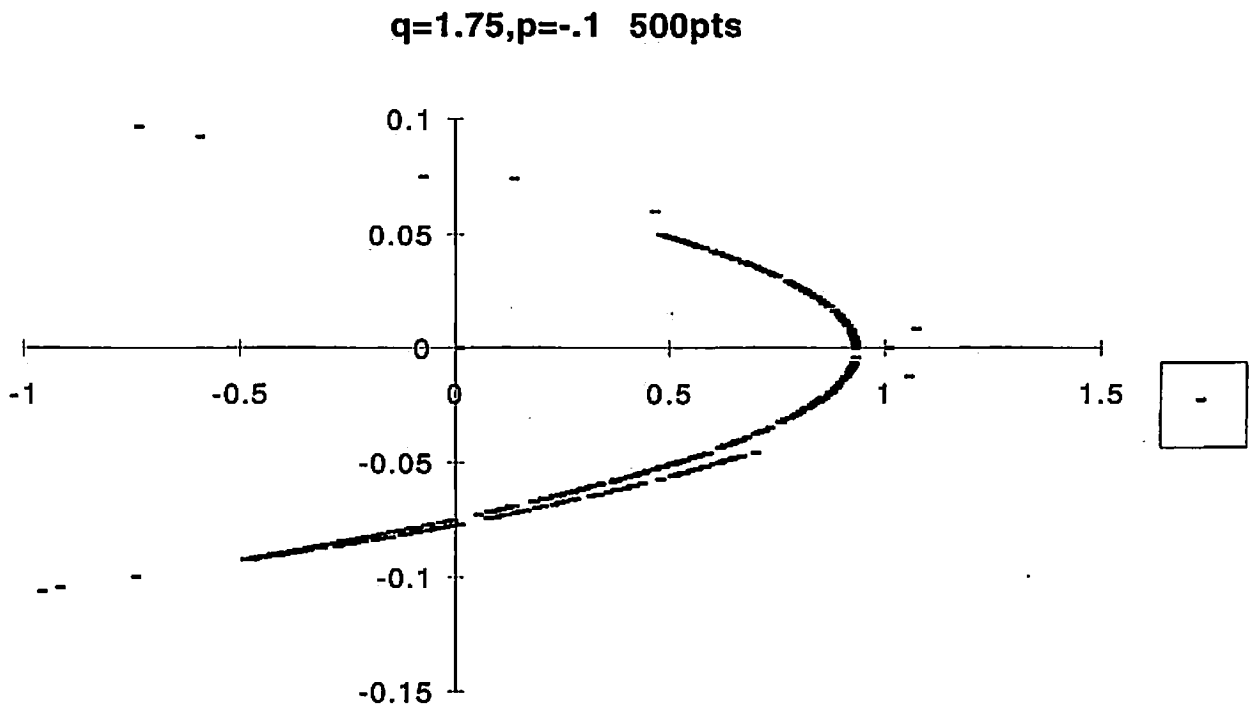

Henon 8

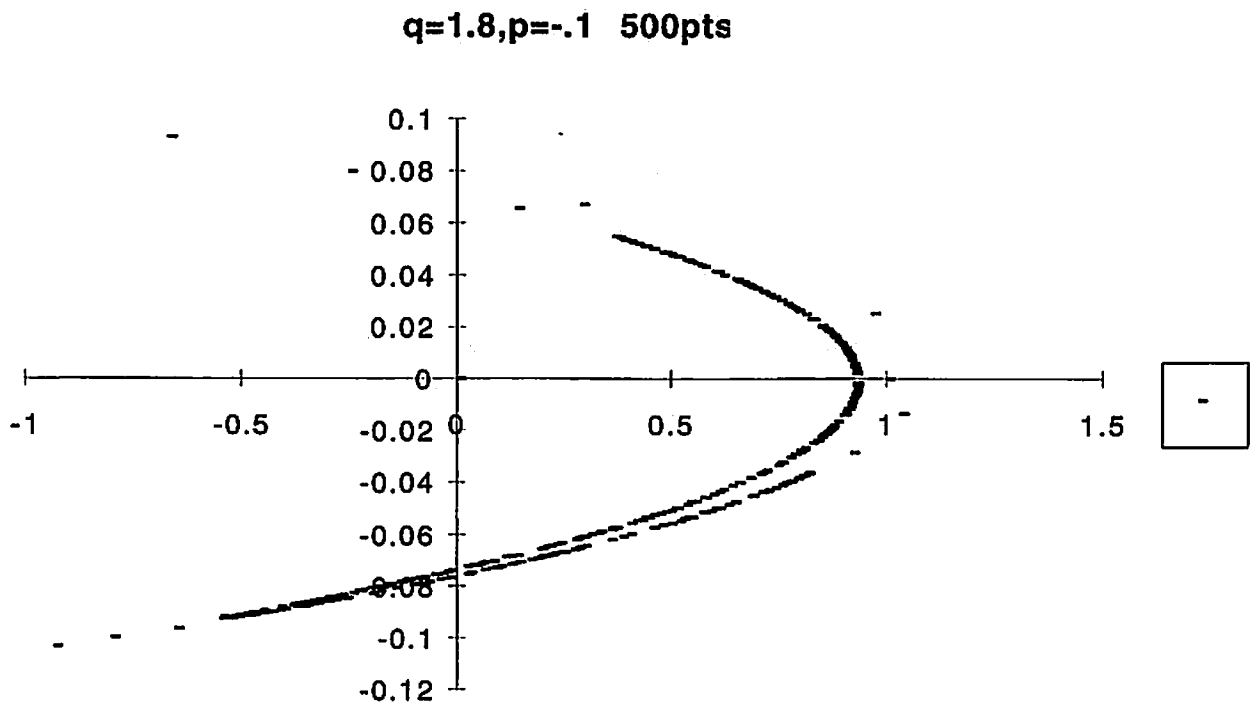
q=1.8,p=-.1 500pts
0.1
0.08
0.06
0.04
0.02
0
-0.02
-0.04
-0.06
-0.08
-0.1
-0.12
-1
-0.5
0
0.5
1
1.5

SIC 1

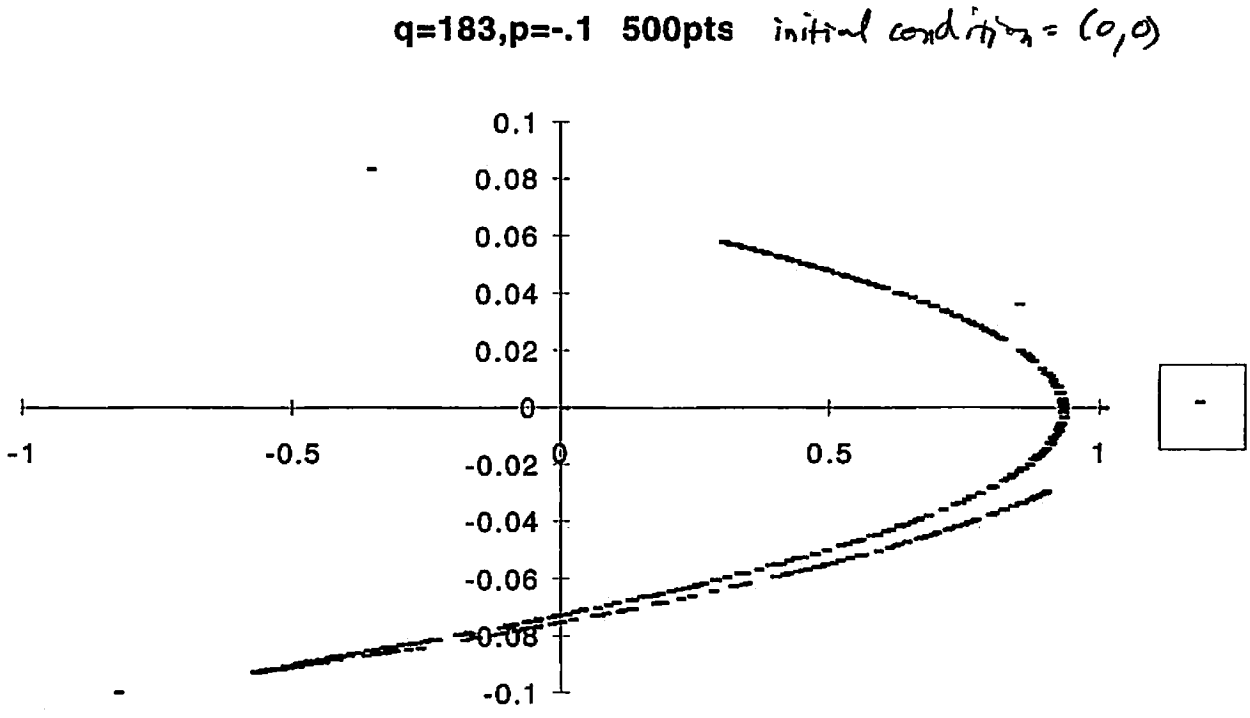
q=183,p=-.1 500pts initial conditions = (0,0)
0.1
0.08
0.06
0.04
0.02
0
-0.02
-0.04
-0.06
-0.08
-0.1
-1
-0.5
0
0.5
1

Sic 2

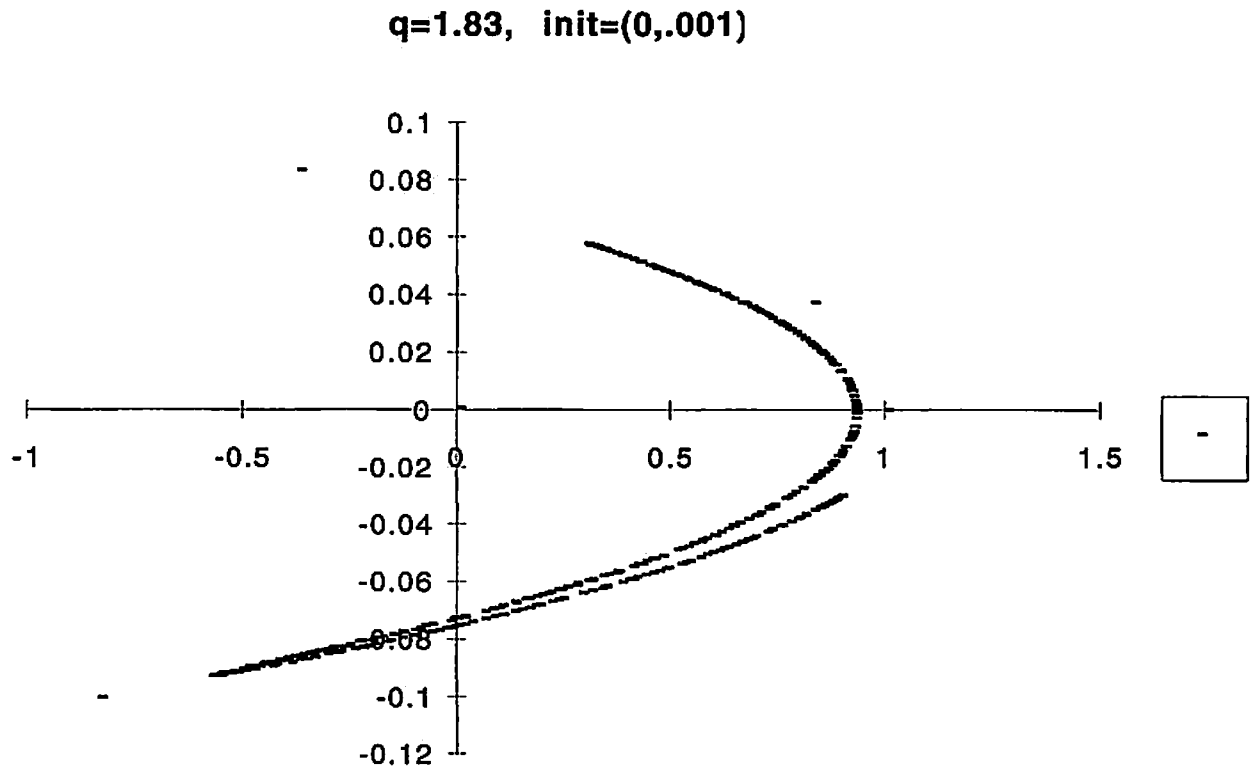
q=1.83, init=(0,.001)
0.1
0.08
0.06
0.04
0.02
0
-0.02
-0.04
-0.06
-0.08
-0.1
-0.12
-1
-0.5
0
0.5
1
1.5

Sic 3

q=1.83, init=(0,.05499)

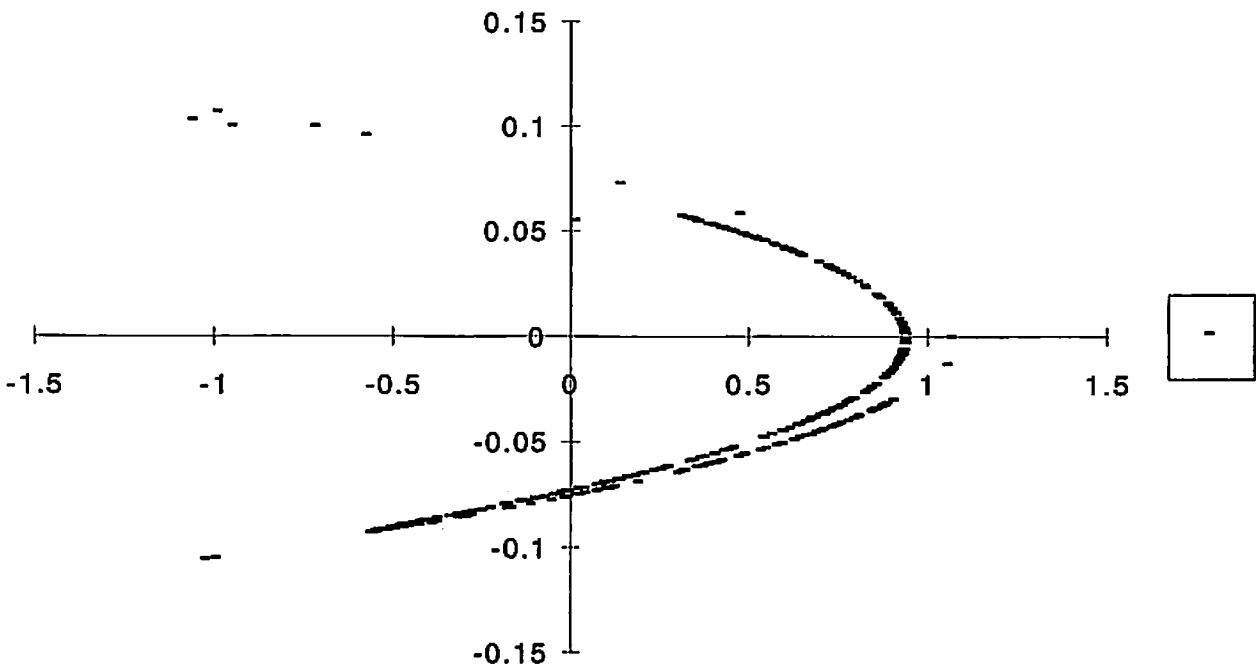

Sic 4

q=1.83, init=(1,1)

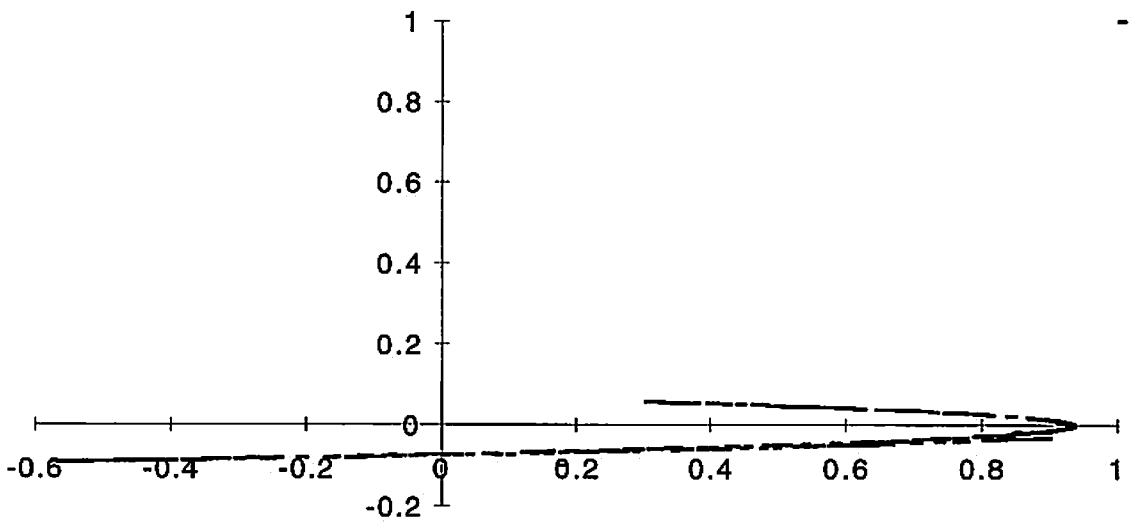

Henon mapping

c−value 1.600000000000000

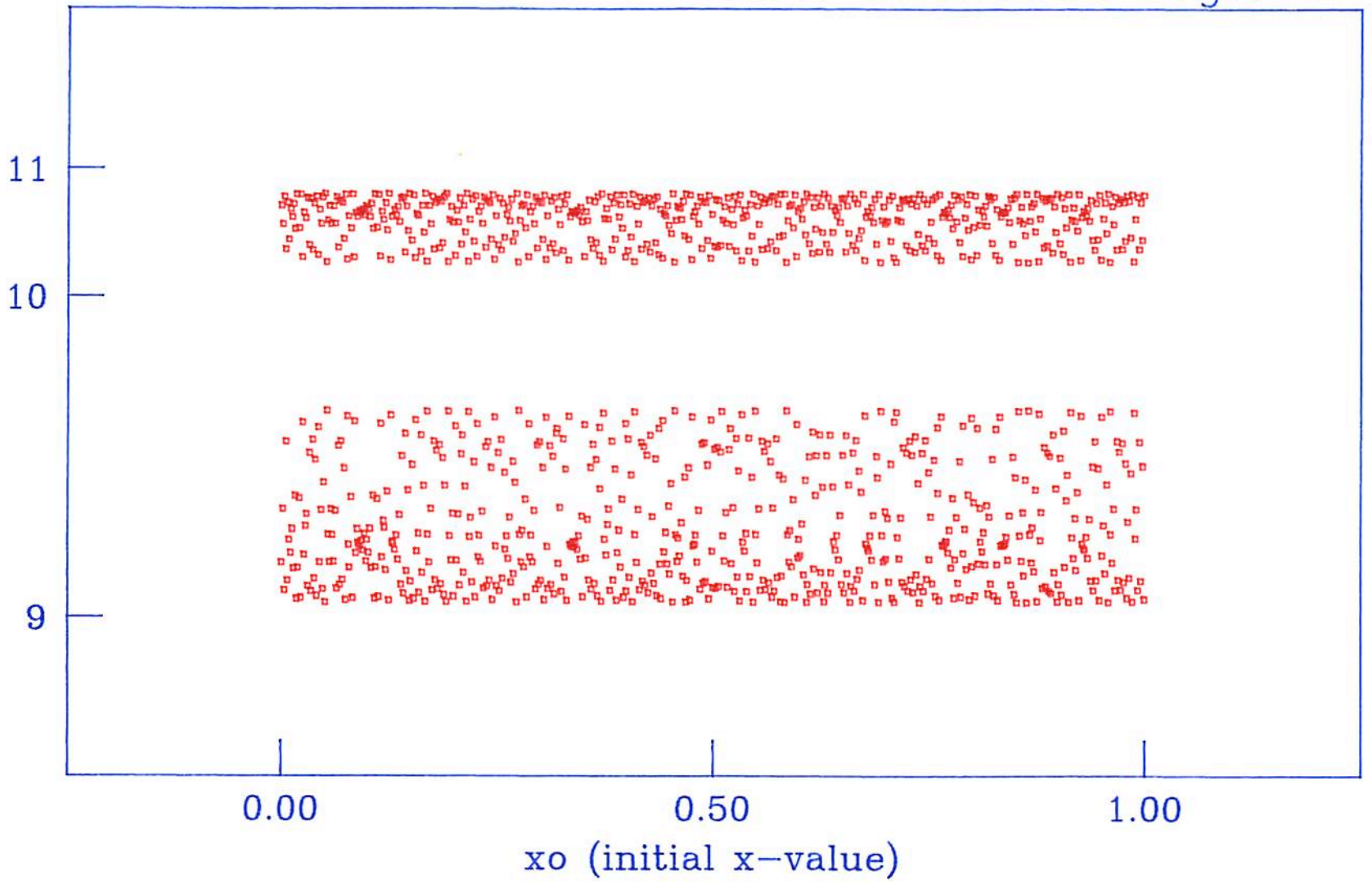

H3

Then I shifted to the IBM. I wrote a fortran program to generate the points of the Henon map, then modified it to generate a series suitable for plotting as a bifurcation diagram. In the program (see appendix 4), what I've been calling the 'q' parameter is referred to as the 'c' parameter. Generally, I would run the program so that it varies the c parameter and stores 10 values of 'x' for every step of 'c'. The resulting bifurcation diagram is represented in figure H2. Again we see the (by now familiar) form that we saw previously in the logistic and circuit bifurcation diagrams. To take a closer look at the chaotic region, I modified the program to keep the 'c' parameter fixed at 1.6, and vary the initial condition of our iteration process. The results are displayed in figure H3. This again shows an observed sensitivity to initial conditions, which is essential to our definition of what constitutes 'chaotic behavior'. By contrast, the mapping of final states versus initial conditions in the period two region does not display this type of sensitivity to initial conditions, converging to the same solutions regardless of where we start the iteration.

It is important to note however, that the determination of the presence of s.i.c. is dependant on the resolution available to the observer. That is, the characterization of a system as sensitive to initial conditions using this method may be more a comment on the limitations of the observer that an objective property of the system. After all, the solutions in figure H3 <u>are</u> limited to the two bands we see. If I couldn't resolve any more than the presence of those two bands, I'd be looking at the same graph as that for the period two region (figure H4). The fact that attribution of the

Henon mapping

c−value 1.200000000000000

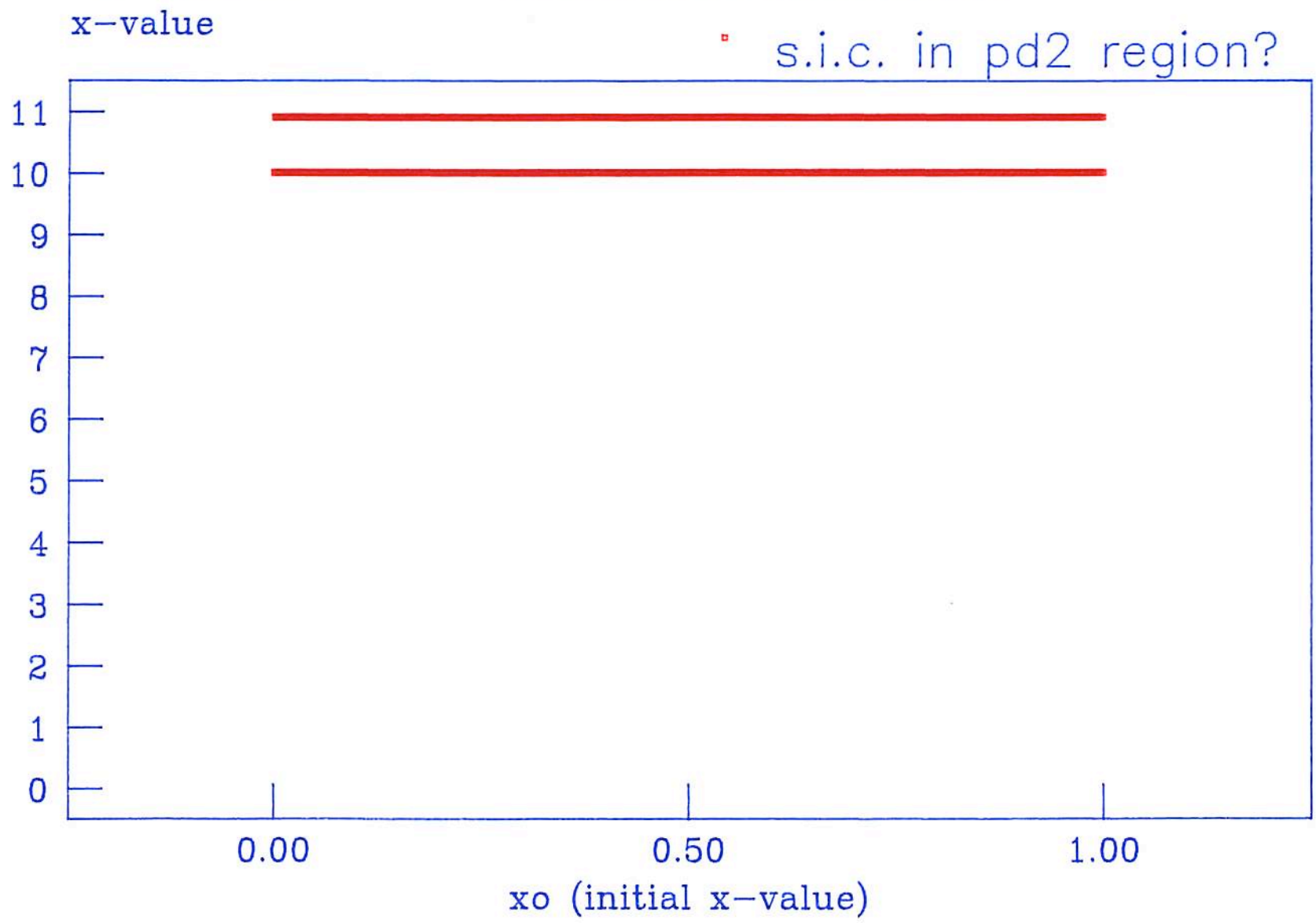

criterion of s.i.c. seems to be relative to the observer is quite important in that its the only factor ruling out Landau's interpretation of this situation as a quasi-periodic system composed of many different frequency oscillations. In this case, we need either a different test or a different criterion.

To get at a different test, I went back to the initial idea of s.i.c. as introduced by Ruelle in Chaotic Evolution and Strange Attractors. The idea is that as time progresses, a small difference in initial conditions can grow exponentially, in which case, "although purely deterministic,... the time evolution is self-independent from its past history and then non-deterministic in any practical sense."

To see if this is indeed what occurs, I went back to the actual raw data of the time series. I first looked to compare the period two and chaotic regions of the logistic map. In the period two region, I saw that even for large differences in initial conditions, the pattern of the time series (that is the sequence in which the particular solutions occurred) converged to the same alternating between the two possible solutions. (See test 1) In the 'chaotic' region, even at small differences in initial conditions, the patterns diverged. That is, even if the two cases had the same myriad of possible solutions, the sequence in which they occurred differed greatly in contrast to the period two region. (See test 2) To make sure that this discrepancy was not due to computation error, I ran the iteration twice for the same initial conditions. The series proved to be identical even past the 500th iteration. (See test 3)

Time Serieses generated by $X_{i+1} = r X_i (1 - X_i)$

Sheet1

r-parameter 3

1	0.9	1	0.1
2	0.27	2	0.27
3	0.5913	3	0.5913
4	0.724993	4	0.724993
5	0.598135	5	0.598135
6	0.721109	6	0.721109
7	0.603333	7	0.603333
8	0.717967	8	0.717967
9	0.607471	9	0.607471
10	0.71535	10	0.71535
11	0.610873	11	0.610873
12	0.713121	12	0.713121
13	0.613738	13	0.613738
14	0.711191	14	0.711191
15	0.616195	15	0.616195
16	0.709496	16	0.709496
17	0.618334	17	0.618334
18	0.707991	18	0.707991
19	0.620219	19	0.620219
20	0.706642	20	0.706642
21	0.621897	21	0.621897
22	0.705423	22	0.705423
23	0.623404	23	0.623404
24	0.704315	24	0.704315
25	0.624767	25	0.624767
26	0.7033	26	0.7033
27	0.626008	27	0.626008
28	0.702366	28	0.702366
29	0.627144	29	0.627144
30	0.701503	30	0.701503
31	0.628189	31	0.628189
32	0.700703	32	0.700703
33	0.629155	33	0.629155
34	0.699957	34	0.699957
35	0.630052	35	0.630052
36	0.69926	36	0.69926
37	0.630887	37	0.630887
38	0.698606	38	0.698606
39	0.631667	39	0.631667
40	0.697991	40	0.697991

Correlation in pattern of time series exhibited depite large difference in initial conditions

Test 1

Time Serieses generated by $x_{i+1} = r x_i (1 - x_i)$

		r-parameter
1	0.1	3.8
2	0.342	
3	0.855137	
4	0.470736	
5	0.946746	
6	0.191589	
7	0.588555	
8	0.9202	
9	0.27904	
10	0.764472	
11	0.684208	
12	0.821056	
13	0.558307	
14	0.937081	
15	0.224049	
16	0.660634	
17	0.851947	
18	0.479305	
19	0.948373	
20	0.186056	
21	0.575468	
22	0.928357	
23	0.252738	
24	0.717674	
25	0.769948	
26	0.673086	
27	0.836156	
28	0.520596	
29	0.948388	
30	0.186003	
31	0.575342	
32	0.92843	
33	0.252503	
34	0.717232	
35	0.770679	
36	0.671585	
37	0.838123	
38	0.515556	
39	0.94908	
40	0.183642	
	0.569686	
	0.931546	
	0.242317	
	0.697678	
	0.801509	
	0.604551	
	0.908463	
	0.316001	

1	0.1001
2	0.342304
3	0.855501
4	0.469751
5	0.946523
6	0.192345
7	0.590325
8	0.918998
9	0.282876
10	0.770857
11	0.671218
12	0.838601
13	0.514328
14	0.94922
15	0.183166
16	0.568541
17	0.932148
18	0.240342
19	0.693796
20	0.807284
21	0.591192
22	0.9184
23	0.284779
24	0.773984
25	0.664745
26	0.846864
27	0.492804
28	0.949803
29	0.181173
30	0.563727
31	0.934568
32	0.232374
33	0.677829
34	0.829832
35	0.536602
36	0.944909
37	0.197812
38	0.602993
39	0.909691
40	0.312182
	0.815953
	0.57066
	0.931027
	0.244019
	0.700999
	0.796477
	0.615985
	0.89888

correlation in time series quickly disappears despite small difference in initial conditions

test 2

r-value = 3.8
Same initial conditions

481	0.893267	481	0.893267
482	0.343227	482	0.343227
483	0.81152	483	0.81152
484	0.55064	484	0.55064
485	0.890768	485	0.890768
486	0.350281	486	0.350281
487	0.819303	487	0.819303
488	0.532964	488	0.532964
489	0.896088	489	0.896088
490	0.335211	490	0.335211
491	0.802241	491	0.802241
492	0.571142	492	0.571142
493	0.88178	493	0.88178
494	0.375279	494	0.375279
495	0.844001	495	0.844001
496	0.473988	496	0.473988
497	0.897564	497	0.897564
498	0.330994	498	0.330994
499	0.797173	499	0.797173
500	0.582078	500	0.582078
501	0.875747	501	0.875747
502	0.39173	502	0.39173
503	0.857799	503	0.857799
504	0.439127	504	0.439127
505	0.88666	505	0.88666
506	0.361779	506	0.361779
507	0.831221	507	0.831221
508	0.505053	508	0.505053
509	0.899908	509	0.899908
510	0.324265	510	0.324265
511	0.788822	511	0.788822
512	0.599696	512	0.599696
513	0.864219	513	0.864219
514	0.422441	514	0.422441
515	0.878344	515	0.878344
516	0.38468	516	0.38468
517	0.852124	517	0.852124
518	0.45363	518	0.45363
519	0.89226	519	0.89226
520	0.346077	520	0.346077
521	0.814708	521	0.814708
522	0.543453	522	0.543453
523	0.893203	523	0.893203
524	0.34341	524	0.34341
525	0.811726	525	0.811726
526	0.550176	526	0.550176

proof that system is still completely deterministic past 500th iteration

test 3

The same test was performed for the Henon recurrence relation. The results were similarly conclusive. (See test 4,5,6)

Acknowledgements:

I would like to thank Damon of 111-lab for use of his analyze program, Mathematica simulation, 2-d chaos explorer, and all the time and expertise he used in answering my questions, Andrew Jewett for the use of his brilliant plotting program that allows relatively easy generation of maps of systems of differential equations, and I'd also like to thank Professor Chua for his time, particularly his explanation of the limitations of the algorithm used in computing Lyupanov exponents from a time series, Professor Judd, Professor Jefferies as well as 111-lab for the use of their equipment, Don Orlando for all his helpful help (irony can be so...ironic) and of course Professor Marsden for his time both during the semester and in reading this monstrosoty.

Time series generated by Henon iteration

0	0	1.3	1	0
1	0	-0.1	-0.3	-0.1
-0.3	-0.1		0.783	0.03
0.783	0.03		0.232984	-0.0783
0.232984	-0.0783		0.851134	-0.023298
0.851134	-0.023298		0.034944	-0.085113
0.034944	-0.085113		0.913299	-0.003494
0.913299	-0.003494		-0.087844	-0.09133
-0.087844	-0.09133		0.898638	0.008784
0.898638	0.008784		-0.041032	-0.089864
-0.041032	-0.089864		0.907947	0.004103
0.907947	0.004103		-0.067576	-0.090795
-0.067576	-0.090795		0.903269	0.006758
0.903269	0.006758		-0.053905	-0.090327
-0.053905	-0.090327		0.905896	0.005391
0.905896	0.005391		-0.06145	-0.09059
-0.06145	-0.09059		0.904501	0.006145
0.904501	0.006145		-0.057415	-0.09045
-0.057415	-0.09045		0.905264	0.005741
0.905264	0.005741		-0.059613	-0.090526
-0.059613	-0.090526		0.904854	0.005961
0.904854	0.005961		-0.058427	-0.090485
-0.058427	-0.090485		0.905077	0.005843
0.905077	0.005843		-0.059071	-0.090508
-0.059071	-0.090508		0.904956	0.005907
0.904956	0.005907		-0.058722	-0.090496
-0.058722	-0.090496		0.905022	0.005872
0.905022	0.005872		-0.058911	-0.090502
-0.058911	-0.090502		0.904986	0.005891
0.904986	0.005891		-0.058809	-0.090499
-0.058809	-0.090499		0.905005	0.005881
0.905005	0.005881		-0.058864	-0.090501
-0.058864	-0.090501		0.904995	0.005886
0.904995	0.005886		-0.058834	-0.090499
-0.058834	-0.090499		0.905001	0.005883
0.905001	0.005883		-0.05885	-0.0905
-0.05885	-0.0905		0.904998	0.005885
0.904998	0.005885		-0.058842	-0.0905
-0.058842	-0.0905		0.904999	0.005884
0.904999	0.005884		-0.058846	-0.0905
-0.058846	-0.0905		0.904998	0.005885
0.904998	0.005885		-0.058844	-0.0905
-0.058844	-0.0905		0.904999	0.005884
0.904999	0.005884		-0.058845	-0.0905
-0.058845	-0.0905		0.904999	0.005885
0.904999	0.005885		-0.058845	-0.0905
-0.058845	-0.0905		0.904999	0.005884
0.904999	0.005884		-0.058845	-0.0905

Correlation in pattern of time series exhibited despite large difference in initial conditions

test 4

Time series Generated by Henon iteration

0	0	1.8	0.001	0
1	0	-0.1	0.999998	-0.0001
-0.8	-0.1		-0.800094	-0.1
-0.252	0.08		-0.252269	0.080009
0.965693	0.0252		0.965458	0.025227
-0.653413	-0.096569		-0.652569	-0.096546
0.134924	0.065341		0.136931	0.065257
1.032573	-0.013492		1.031507	-0.013693
-0.932665	-0.103257		-0.928904	-0.103151
-0.669014	0.093267		-0.656304	0.09289
0.287623	0.066901		0.317568	0.06563
0.917993	-0.028762		0.884101	-0.031757
-0.545642	-0.091799		-0.4387	-0.08841
0.372296	0.054564		0.565165	0.04387
0.805077	-0.03723		0.468929	-0.056517
-0.203897	-0.080508		0.547674	-0.046893
0.844659	0.02039		0.413203	-0.054767
-0.263818	-0.084466		0.637907	-0.04132
0.790254	0.026382		0.226214	-0.063791
-0.097722	-0.079025		0.844098	-0.022621
0.903785	0.009772		-0.305125	-0.08441
-0.460518	-0.090379		0.748008	0.030512
0.527883	0.046052		0.023383	-0.074801
0.544463	-0.052788		0.924215	-0.002338
0.41362	-0.054446		-0.53985	-0.092421
0.637607	-0.041362		0.382989	0.053985
0.226861	-0.063761		0.789959	-0.038299
0.843601	-0.022686		-0.161564	-0.078996
-0.303678	-0.08436		0.874019	0.016156
0.749644	0.030368		-0.35888	-0.087402
0.018829	-0.074964		0.680767	0.035888
0.924397	-0.001883		0.20169	-0.068077
-0.540002	-0.09244		0.858701	-0.020169
0.382676	0.054		-0.347431	-0.08587
0.790406	-0.038268		0.696854	0.034743
-0.162803	-0.079041		0.160652	-0.069685
0.873251	0.01628		0.883858	-0.016065
-0.356339	-0.087325		-0.422235	-0.088386
0.684115	0.035634		0.590707	0.042223
0.19321	-0.068411		0.414142	-0.059071
0.864394	-0.019321		0.632205	-0.041414
-0.364241	-0.086439		0.239156	-0.063221
0.674753	0.036424		0.833827	-0.023916
0.2169	-0.067475		-0.275398	-0.083383
0.847842	-0.02169		0.780098	0.02754
-0.315596	-0.084784		-0.067855	-0.07801
0.735934	0.03156		0.913702	0.006786
0.056681	-0.073593		-0.495948	-0.09137

Correlation in time series quickly disappears despite small difference in initial conditions

time series generated by Henon iteration

$p = 1.8$
$q = -.1$
same initial conditions

	-0.511522	-0.091371	-0.511522	-0.091371
	0.437651	0.051152	0.437651	0.051152
	0.706383	-0.043765	0.706383	-0.043765
	0.058076	-0.070638	0.058076	-0.070638
	0.923291	-0.005808	0.923291	-0.005808
	-0.540245	-0.092329	-0.540245	-0.092329
	0.382314	0.054025	0.382314	0.054025
	0.79093	-0.038231	0.79093	-0.038231
	-0.164257	-0.079093	-0.164257	-0.079093
	0.872342	0.016426	0.872342	0.016426
491	-0.35334	-0.087234	-0.35334	-0.087234
492	0.688037	0.035334	0.688037	0.035334
493	0.183222	-0.068804	0.183222	-0.068804
494	0.870769	-0.018322	0.870769	-0.018322
495	-0.383153	-0.087077	-0.383153	-0.087077
496	0.648672	0.038315	0.648672	0.038315
497	0.280921	-0.064867	0.280921	-0.064867
498	0.793083	-0.028092	0.793083	-0.028092
499	-0.160258	-0.079308	-0.160258	-0.079308
500	0.874463	0.016026	0.874463	0.016026
501	-0.360409	-0.087446	-0.360409	-0.087446
502	0.678744	0.036041	0.678744	0.036041
503	0.206794	-0.067874	0.206794	-0.067874
504	0.855151	-0.020679	0.855151	-0.020679
505	-0.336989	-0.085515	-0.336989	-0.085515
506	0.710074	0.033699	0.710074	0.033699
507	0.12613	-0.071007	0.12613	-0.071007
508	0.900357	-0.012613	0.900357	-0.012613
509	-0.471769	-0.090036	-0.471769	-0.090036
510	0.509345	0.047177	0.509345	0.047177
511	0.580198	-0.050935	0.580198	-0.050935
512	0.343132	-0.05802	0.343132	-0.05802
513	0.730049	-0.034313	0.730049	-0.034313
514	0.006339	-0.073005	0.006339	-0.073005
515	0.926923	-0.000634	0.926923	-0.000634
516	-0.547168	-0.092692	-0.547168	-0.092692
517	0.3684	0.054717	0.3684	0.054717
518	0.810424	-0.03684	0.810424	-0.03684
519	-0.219056	-0.081042	-0.219056	-0.081042
520	0.832584	0.021906	0.832584	0.021906
521	-0.225846	-0.083258	-0.225846	-0.083258
522	0.82493	0.022585	0.82493	0.022585
523	-0.202332	-0.082493	-0.202332	-0.082493
524	0.843818	0.020233	0.843818	0.020233
525	-0.261418	-0.084382	-0.261418	-0.084382
526	0.792607	0.026142	0.792607	0.026142
527	-0.104665	-0.079261	-0.104665	-0.079261
528	0.901021	0.010467	0.901021	0.010467

test 6

APPENDIX #1
Block DIAGRAM OF SYSTEM APPARATUS

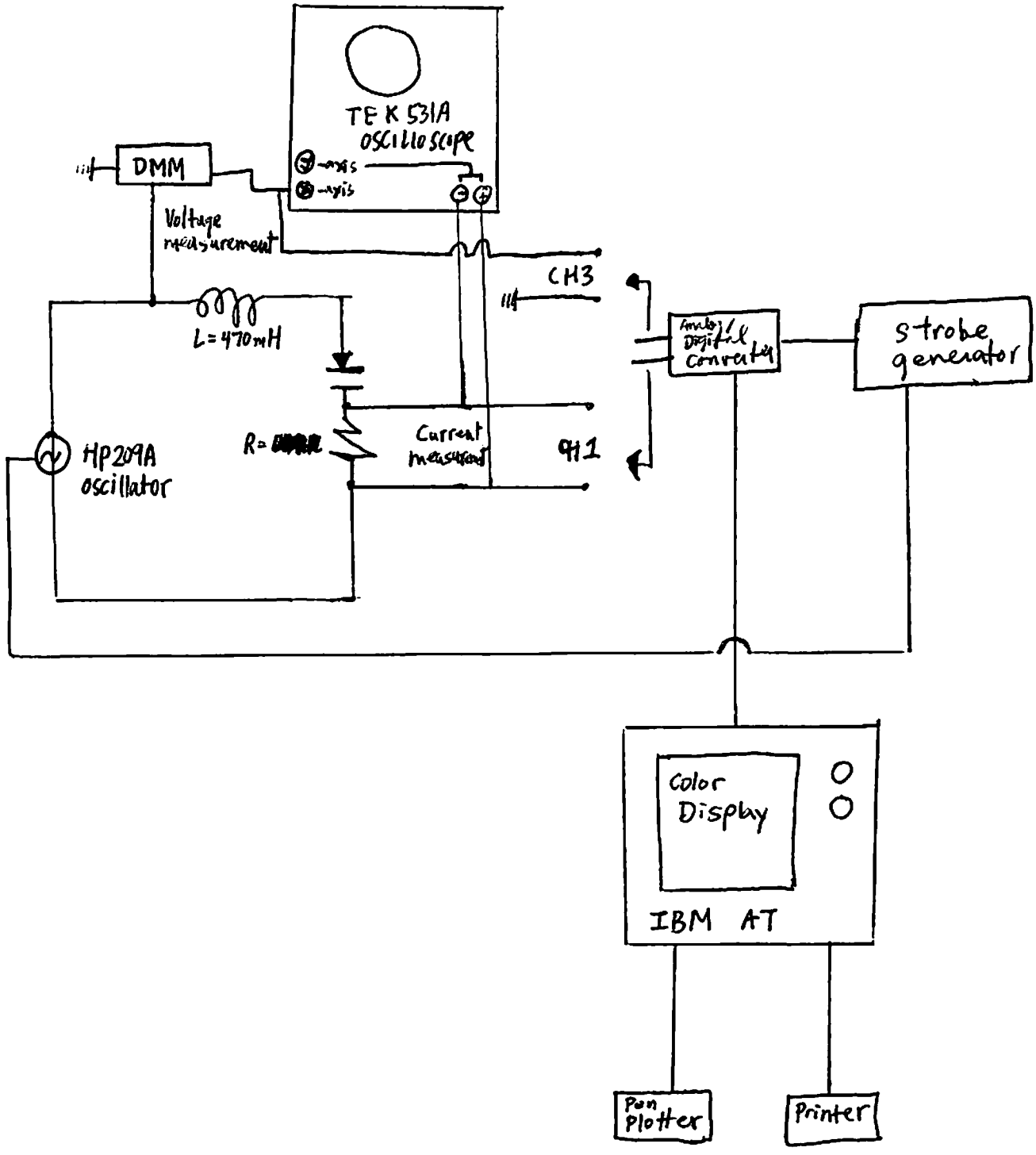

Appendix 3

```
      PROGRAM FFFT
C     FAST FOURIER PGM. FOR FORTRAN 2.0 COMPILER (FILENAME FFPP.FOR)
C     THIS PGM CALCS,SCALES AND OUTPUTS LOG POWER VS FREQ,DOES NOT PLOT.
$NOFLOATCALLS
C     REVISED 07/06/1986 10:04:33; INPUT N=NO. OF POINTS
C     THIS PGM.RECEIVES AND PASSES PARAMETERS AND DATA BY DOS REDIRECTION.
C     PARAMETERS ON FIRST LINE;DATA ON NEXT N LINES.
      DIMENSION EDATA(2,1024),PDATA(1024),X(1024),Y(1024)

      READ(*,56)N,CC,DD,EE,FF,GG,HH,BB
   56 FORMAT(I6,F16.5,F10.4,F10.4,F10.4,F10.4,F10.4,F10.4)
      DO 15 I=1,N
      READ(*,55)EDATA(1,I)
   55 FORMAT(F16.6)
      EDATA(2,I)=0
   15 CONTINUE
C     CALL FFT SUBROUTINE FOR REAL(ONLY) DATA.SEE:E.O.BRIGHAM,PAGE 164.
      CALL FFT(EDATA,N)
      RMAX=0
      DO 25 I=1,N
      PDATA(I)=EDATA(1,I)**2 +EDATA(2,I)**2
      IF (PDATA(I) .GT.  RMAX) RMAX=PDATA(I)
   25 CONTINUE
      WRITE(*,27)N,RMAX,DD,EE,FF,GG,HH,BB
   27 FORMAT(I6,F16.5,F10.4,F10.4,F10.4,F10.4,F10.4,F10.4)
      DO 26 I=1,N
      IF (PDATA(I) .LT. RMAX*1.0E-10) PDATA(I)=RMAX*1.0E-10
      Y(I)=-ALOG10((PDATA(I))/ABS(RMAX))
      WRITE(*,57)Y(I)
   57 FORMAT(F16.6)
   26 CONTINUE
      END
C     RUN USING DOS REDIRECTION: C>_ FFTC.EXE < DATA.IN > DATA.OUT
C     IN DATA.IN FILE,FIRST LINE IS VALUE OF N (USE POWER OF 2) ,
C     SECOND LINE IS VALUE OF EDATA(1,1) ,ETC.

      SUBROUTINE FFT(XDATA,N)
      DIMENSION XDATA(2,N)
      DO 104 M=1,12
      L=2**M
      IF (L  .EQ.  N)   NU=M
  104 CONTINUE
      N2=N/2
      NU1=NU-1
      K=0
      DO 100 L=1,NU
  102 DO 101 I=1,N2
      P=FLOAT(IBITR(K/2**NU1,NU))
      ARG=6.283185307I*P/FLOAT(N)
      C=COS(ARG)
      S=SIN(ARG)
      K1=K+1
```

```
      K1N2=K1+N2
      TREAL=XDATA(1,K1N2)*C+XDATA(2,K1N2)*S
      TIMAG=XDATA(2,K1N2)*C-XDATA(1,K1N2)*S
      XDATA(1,K1N2)=XDATA(1,K1)-TREAL
      XDATA(2,K1N2)=XDATA(2,K1)-TIMAG
      XDATA(1,K1)=XDATA(1,K1)+TREAL
      XDATA(2,K1)=XDATA(2,K1)+TIMAG
  101 K=K+1
      K=K+N2
      IF (K.LT.N) GO TO 102
      K=0
      NU1=NU1-1
  100 N2=N2/2
      DO 103 K=1,N
      I=IBITR(K-1,NU)+1
      IF (I.LE.K) GO TO 103
      TREAL=XDATA(1,K)
      TIMAG=XDATA(2,K)
      XDATA(1,K)=XDATA(1,I)
      XDATA(2,K)=XDATA(2,I)
      XDATA(1,I)=TREAL
      XDATA(2,I)=TIMAG
  103 CONTINUE
      RETURN
      END
      FUNCTION IBITR(J,NU)
      J1=J
      IBITR=0
      DO 200 I=1,NU
      J2=J1/2
      IBITR=IBITR*2+(J1-2*J2)
  200 J1=J2
      RETURN
      END
```

Appendix 4

```
c23456789
c
c       This program calculates points of a Henon map, suitable
c       for use in
c       plotting a time series or two dimensional return map.  The
c       program
c       requires as input the parameters C and J, the starting
c       values XINIT
c       and YINIT, the number of preiterations P to perform, and
c       the number
c       of iterations I to perform.  Output is a series of
c       consecutive x
c       values suitable for piping to PRM01.  If y(n+1) is
c       required, it can
c       be obtained by multiplying x(n) by J.
c
c        By dan ernst  nov 13, 1993.
c
c
C       PROGRAM HENON
        REAL*8 C, J, X, Y, X1, Y1, xsum, xo, yo
        INTEGER P, I, N, q, m
        open (8,FILE='dan.dat')
C
C       TYPE C, J, INITIAL X, INITIAL Y, P, AND I
        READ(*,*) C, J, X, Y, P, I
C
           xo=x
           yo=y
C       PERFORM PREITERATIONS
            q=0
         write (8,*) 100*p
  5      if (q .le. 100) then
C       PERFORM preITERATIONS AND SEND DATA STREAM
         n=0
         m=0
 50     if (n .le. 20) then
```

```
            X1 = 1 - C*X*X + Y
            Y1 = J*X
            Y = Y1
            X = X1
            N = N + 1
            GOTO 50
          ENDIF
 10     if (m .le. p) then
          X1 = 1 - C*X*X + Y
          Y1 = J*X
          Y = Y1
          X = X1
           write(8,*) c,x + 10.0
          m = m + 1
          GOTO 10
         ENDIF
          q=q+1
          c=c+.02
          goto 5
         ENDIF
C
C       PERFORM ITERATIONS AND SEND DATA STREAM
c        N = 0
c        WRITE (*,*) I, 0.0, C
C 15    FORMAT (I10, D16.12, D16.12)
C 20    FORMAT (D16.12)
c 30     IF (N .LE. 100) THEN
c        WRITE (*,*) X
c          X1 = 1 - C*X*X + Y
c          Y1 = J*X
c          Y = Y1
c          X = X1
c          N = N + 1
c          GOTO 30
c       ENDIF
C
        close (8)
        END
                        ^Z^Z^Z^Z^Z^Z^Z^Z^Z^Z^Z^Z^Z^Z
```

PART II

Brain Section

There is a great deal of research being done currently on the connection between 'chaos' understood (perhaps mis-understood) in the technical sense, and brain activity. The naive idea is that where once we saw only randomness and irregularity, there might be order and deterministic regularity after all. Unfortunately, this naive conception of what chaos theory implies is all too clearly a part of the working assumptions in much of the research I've come across. There is, however, a good deal of work being done that does seem grounded in a solid understanding of the mathematics involved, particularly that of Walter J. Freeman. After becoming disillusioned with much of the literature (I'll use Babloyantz' work as an example here) my excitement was sparked anew when I ran across Freeman's work. I paid particular attention to the work he's been doing, and the bulk of this paper will address itself to this topic.

A. Babloyantz and D. Gallez of the Universite Libre de Bruxelles, have done a good deal of work in the field, their results are cited quite often, their criticism appears regularly in feedback publications such as Behavioral and Brain Sciences. In their recent "Predictability of the human EEG: a dynamical approach"[1], they looked at electroencephalogram recordings from the human scalp. Three stages of brain activity were considered: alpha waves (awake with eyes closed), deep sleep, and the Creutzfeld-Jacob coma. Fitting the recorded time serieses to deterministic equations, the Lyapunov exponents were measured, and the Kolmogorov metric entropy was determined. From the presence of positive Lyapunov exponents in "periodic" time serieses, they postulate that

the EEG's behavior is chaotic. Since the metric entropy can be used to determine the rate at which information is lost in a system, they used the inverse of the Kolmogorov entropy to determine the "predictability time".

Their findings can be summarized in Figure 1. The CJ coma time series is labeled as a 1.4 Hz "hyperchaotic attractor" since it has more than one positive Lyapunov exponent. The alpha wave trace is similarly labeled a 10 Hz "hyperchaotic attractor". For the time being, we'll ignore that the notion of chaotic behavior with a definite frequency seems seriously confused. Rather than admit that perhaps there is no particular chaotic attractor correlated with the mental state of "deep sleep", they label the irregular trace recorded during "deep sleep" as having a "pseudo-cycle of 1 Hz" and claim that "due to limited data, the attractor is not represented adequately".

Babloyantz' main thrust seems to be that there is a particular and determined chaotic attractor correlated with each identifiable mental state. Rather than deal with the implausible implications of this view on logical grounds, I'd like to point out some of the problems with this conclusion on its own terms.

> "The first step in the dynamical analysis reported is the construction of the phase space. The variables responsible for the EEG activity are not known. However, from a single measured property, V(t), a set of variables can be constructed by introducing a time delay, T, leading to the $V(t),V(t+T),\ldots,V(t+(d_e-1)T)$ variables." p383

First of all, Babloyantz' phase portrait of the variables is just a 2-D return map of the time series. Because the first and third return maps in fig.1 show some regularity and not exact periodicity, Babloyantz thinks they are chaotic attractors. Really,

Figure 1 - From Babloyantz

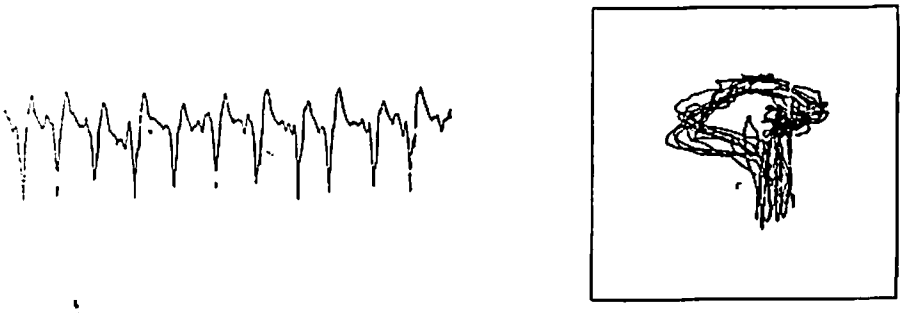

(a) CJ COMA

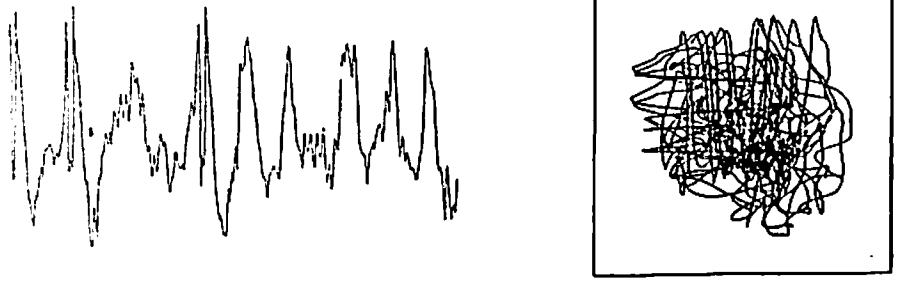

(b) DEEP SLEEP

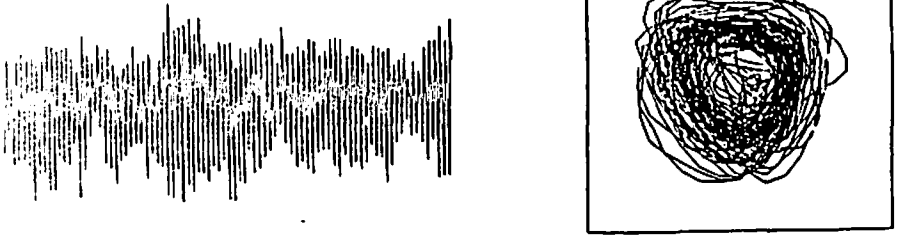

(c) ALPHA RHYTHM

Fig. 1. Short stretches of three stages of human EEG activity together with the corresponding phase portraits. The EEG were recorded on an analog tape and processed off-line (signal digitized in 12 bits, 250 Hz sampling frequency). The phase portraits are reconstructed by the time-delay method (τ = 104 ms, 170 ms and 24 ms respectively for CJ coma, deep sleep and alpha rhythm)

they just represent the time series in another way, and show the same thing- either the trace is irregular or vaguely periodic.

Furthermore, It is not at all clear that the evaluation of Lyapunov exponents and Kolmogorov entropies means anything in the cases considered. Babloyantz argues that "any attractor exhibiting one positive Lyapunov exponent is a chaotic attractor". Positive characteristic exponents are a measure of the rate of divergence of trajectories in phase space, and negative are a measure of the convergence. But to talk about such exponents assumes there is a causal connection between the first and next point in the time series (phase space trajectory)- this is not necessarily what is going on in EEG activity, and there is nothing in Babloyantz' paper to give evidence that it is. In fact this is the interesting and vital question at stake in these investigations, but it seems Babloyantz assumes a priori that there is a chaotic attractor for a particular human mental state. In a tangled web of circular logic, he uses the conclusion as an assumption to derive the conclusion. He "relates the static and dynamic properties of the attractor" to demonstrate that there is an attractor.

One of Babloyantz' major findings is that

> "the dynamical silhouette of the attractor is unchanged.
> (i) The absolute values of the positive exponents may vary from one individual to another, but are similar for two different recordings from the same individual at two years interval.
> (ii) The negative exponents are remarkably stable from one individual to another as well as for different recordings of the same individual." p387

But of course this is so! The phase space referred to is just another representation of the time series. The very reason why a particular EEG trace is identified as "alpha-waves" is because of

its familiarity. It is a pattern seen in different individuals exhibiting the same behavior- that is why we have the classification 'alpha-wave'. The interesting question is what this commonality implies, not that it exists.

I believe that Babloyantz' assumptions may stem from a misunderstanding of other work done in this field. As support for his assumptions, he makes the claim that "in all cases, the analysis has shown the presence of chaotic attractors". He cites specifically the works of Skarda and Freeman. And we'll see that their work does not make that claim, rather they are merely exploring the possibility of modeling EEG activity by a chaotic system. Babloyantz also writes "different algorithms allow the evaluation of Lyapunov exponents from experimental time series", citing Eckmann(1986)[3]. He fails to point out the distinction that these algorithms determine the exponents by means of fitting the data to equations, the exponents are of a deterministic simulation of the time series that presupposes a causal relationship that may not be present in the actual data.

These unsupported assumptions lead Babloyantz to several conclusions that strike me as unfounded even in the context of his assumptions.

> "A small value of K is observed for deep sleep, which corresponds to a large predicting time. In this state, the brain waves are slow in exploring new possibilities or defining new codings of information. It is therefore legitimate to characterize this state of the brain as a poor cognitive state. The low degree of entropy/chaos may be related to the slow processing of information during the deep sleep" p388

Conclusions such as this, and similar ones concerning the other two states examined, seem to me premature with respect to the data

presented in Babloyantz' paper, and misguided in relation to other work such as Eeckman, Skarda, Rapp, and Freeman's.

In "Asymmetric sigmoid non-linearity in the rat olfactory system"[7] Freeman similarly looks at EEG traced during four physical states of the brain: Seizure, motivation, waking rest, and deep anesthesia. The traces are displayed in figure 2. EEG probes were surgically implanted in the three layers of the rat central olfactory system. Using precise methodology, signals could be localized to the olfactory bulb (OB), anterior nucleus (AON), and prepyriform cortex (PC). Each of these masses has been investigated extensively in previous work (Freeman 1975, Freeman 1979, Eeckman Freeman 1990, Bressler 1987)[4,5,8,2] and shown to contain both inhibitory and excitatory neurons. The existence of these two different classes of neurons makes possible a model of the system as partially a negative feedback loop rather than a simple coupled oscillator model. Division of the population of neurons into two distinct categories is further supported by Rapp, and Zimmerman's classic work, "Dynamics of Spontaneous Neural Activity in the Simian Motor Cortex: the Dimension of Chaotic Neurons"[12] In their work Rapp and Zimmerman looked at the spontaneous activity of 10 individual neurons, in the brain of a severely disabled (anesthetized, artificially respired, post craniotomy and pneumothorax) monkey. Table 1, shows that there are two populations of neurons. One that as expected has high dimension. The other with low dimensional activity.

> "It would have been difficult to justify an a priori speculation that a low dimensional dynamical system describing the activity of <u>any</u> central nervous system neuron could possibly exist. Yet evidently this is indeed the case.

Figure 2 - From Freeman

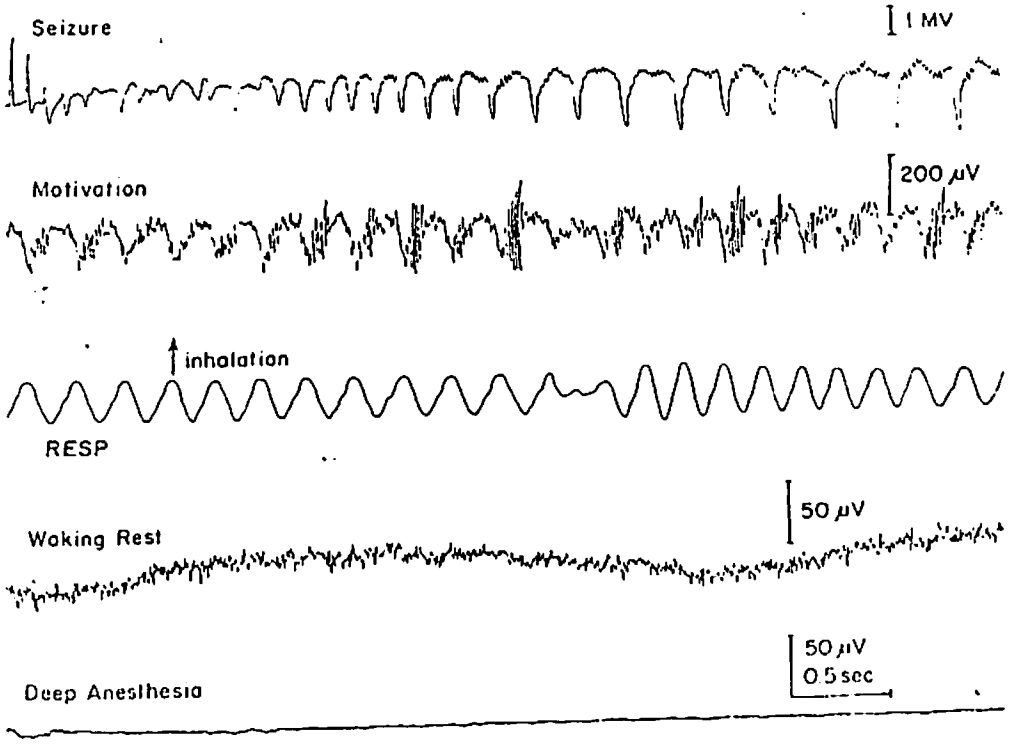

Four basic states of olfactory EEG (from Freeman[8], with permission). The explanation is in the text.

TABLE 1 - 10 individual neurons activity and trace dimensio

Table 1

Neuron	Location	Dimension	Peak (ms)	FWHM (ms)
A	postcentral	3.5 ± 0.1	21	40
B	postcentral	high	2	<5
C	postcentral	very high	2	<5
D	precentral	high	1	5
E	postcentral	high	1	5
F	precentral	high	5	10
G	precentral	2.9 ± 0.1	32	40
H	postcentral	2.2 ± 0.1	17	25
I	postcentral	ambiguous	6	25
J	postcentral	ambiguous	5	10

From Rapp (1985)

Neurons in this structurally complex system can on occasion display comparatively simple dynamical behavior." p335

This early work led to further investigation, specifically Freeman's "Correlations between unit firing and EEG in the rat olfactory system"[8], where a 1/4 period phase shift is measured between the responses of two populations of neurons. The inhibitory granule cells are observed, as predicted by Freeman's negative feedback hypothesis, to follow the pyramidal excitatory cells by a phase difference of pi/2. As we shall soon see, negative feedback is one of the key points to Freeman's model.

Experiments with both rats and rabbits show that there is a continuous sustained background of non-periodic behavior in the olfactory system EEG. This background was studied at great length, and shown to be quite robust- enduring all but the most drastic of measures such as near-lethal levels of anesthesia. However, periodic behavior is observed naturally, in induced seizures, and in transient "bursts" that accompany the introduction of conditioned stimulus (CS). "During odor application the frequency and duration of the bursting periods increases."[8] Freeman realizes that with the advent of chaos theory, we now know that we can devise a single deterministic model that will exhibit both types of behavior observed (non-periodic, and periodic).

The success of his model in simulating the observed EEG is remarkable. As mentioned before, there are three main parts of the central olfactory system, the OB, PC, AON, each made up of both excitatory and inhibitory neurons. Each mass of neurons is modelled in its non-interactive state as a second order ODE. In the non-interactive state, the model is called KO_e for "open loop"

excitatory neurons and KO_i for inhibitory. Coupled KO sets are represented as KI_e or KI_i, with KII being the system where both the inhibitory and excitatory KI sets for a particular part of the olfactory system (OB, AON, or PC) are coupled. The KII set is sufficient for modelling the behavior of any one part separately. The KIII set is formed by the coupling of all three KII sets and is sufficient to simulate the chaotic patterns of the observed olfactory EEG. Including "normal low-level background activity, high-level relatively coherent 'bursts' of oscillation that accompany reception of input into the bulb, and a degenerate epileptic state determined by a toroidal chaotic attractor"[6]

The model takes into account differential velocities and separation between axons in the actual AON,PC, and OB. At each stage of the coupling there is a gain parameter, k_{ij}. Increasing one of any number of gain parameters in the KIII model demonstrates the Ruelle-Takens-Newhouse route to chaos. KIII (which is the sum of all the feedback connections between the three KII sets) can be characterized by a parameter matrix.

The model's correspondence to observed data is exceptional. KIII exhibits self-sustained excitation, unlike any of the KI, or KII sets which need maintained external stimulation to sustain activity. Delayed feedback from the KII_{AON} to the KI_{PC} set keeps excitation chaotic (non-periodic). See figure 3. Also, remarkably, the KIII model responds to external stimulation with near-periodic "bursts" characteristic of EEG during inhalation (which is a period of increased input stimulation). See Figure 4.

Fig 3, 4, 5 Comparison of actual and simulated EEG Traces

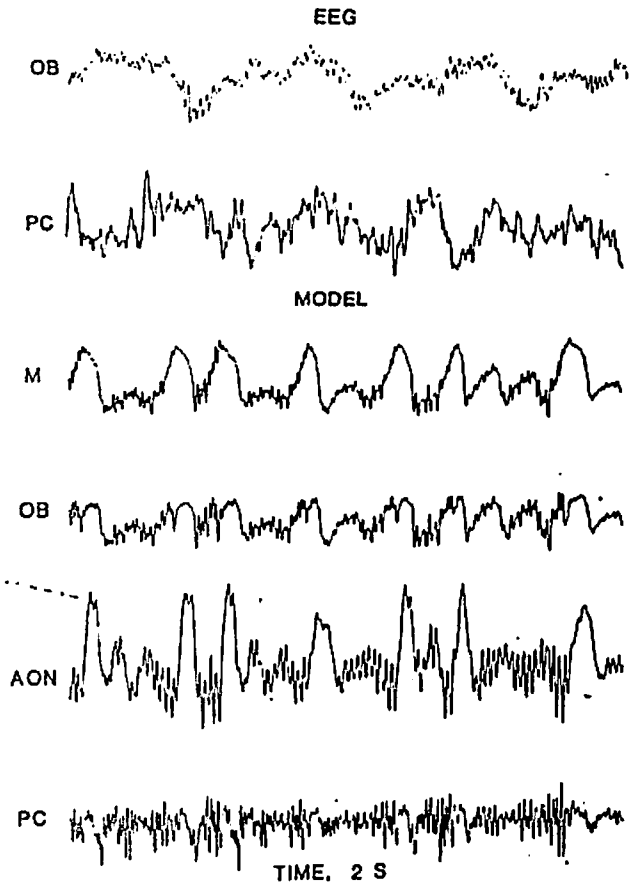

Fig. 3. Examples of chaotic background activity generated by the model, simulating bulbar unit activity (M) and the EEGs of the OB, AON and PC. $Q_m = 5.0$, $k_{ME} = 1.5$, $k_{EG} = 0.67$, $k_{EP} = 1.0$, $k_{PM} = 0.1$, $k_{MA} = 1$, $k_{EA} = 1.5$, $k_{AI} = 1.0$, $k_{AP} = 1$. The *top two traces* are representative records of the OB and PC EEGs from a rat at rest breathing through the nose

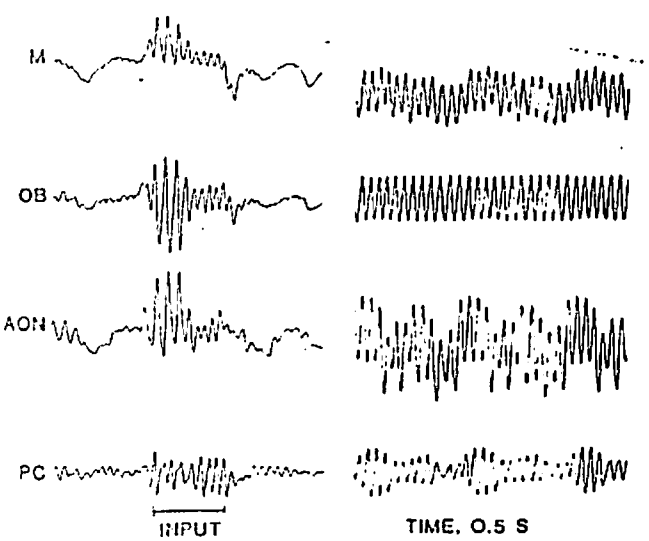

Fig. 4 *Left*: a simulated burst induced by giving a surge of input at R similar to receptor input density during inhalation and exhalation lasting 0.2 s. *Right*: sustained input onto pre-existing chaotic activity

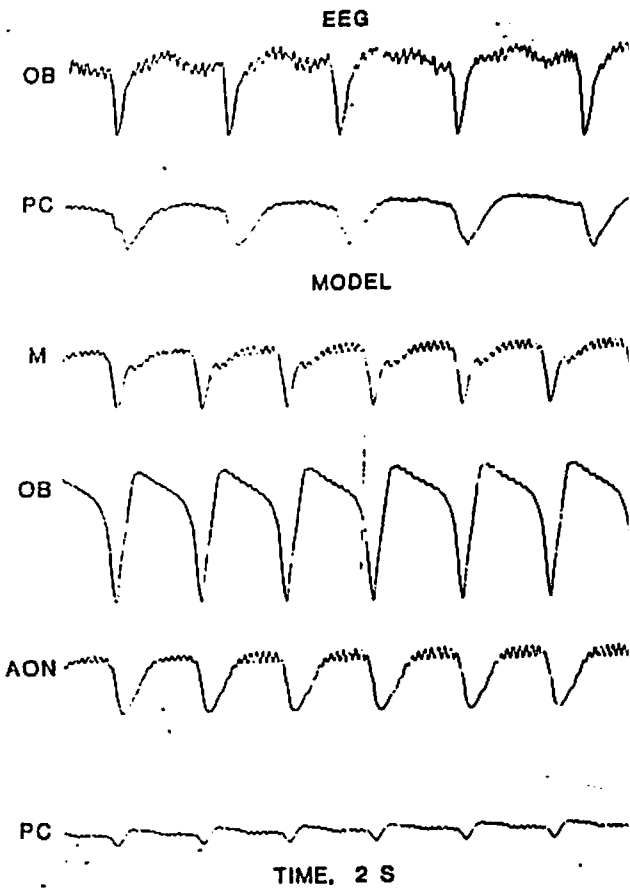

Fig. 5 Examples of 2-s time segments of EEGs recorded from rat during a seizure, comparing these with the outputs of t model (see Fig. 3)

From Freem (1987)

Three changes in the KIII model are needed for seizure modelling.

1) the input to the PC from the KII_{AON} and the KII_{PC} sets must be reduced to 20% its normal level.
2) feedback from KII_{PC} to the KII_{AON} sets must be reduced.
3) feedback from the AON to the OB must be increased.

Each of these requirements can be achieved by varying one gain parameter. With these settings in place, even a small pulse will initiate periodic behavior that continues indefinitely, thus simulating seizure. See figure 5.

"KIII is a simplification serving to emphasize the capacity for generating chaotic background activity."[6] The success of the model in simulating the observed types of EEG is indisputable, however there are many questions left unanswered.

According to Freeman, "The results suggest that a 'learned' patterned attractor is formed by synaptic modification in the OB for each discriminable odor."[6] These thoughts are echoed in other papers, "Learning consists in the selective strengthening of excitatory connections to form ... a global state manifesting an attractor."[10] Presumably, these would be latent after exhalation and come into existence with each inhalation. That is, he is postulating the existence of a static mosaic of basins in the olfactory bulb. "We conceive that the receptor input to the OB is determined by the odor stimulation which selects the basin for the appropriate attractor."[6] This conception calls for a rethinking of current 'brain as computer' models of information manipulation. In this view of learning there is no program-specified rule necessary for any identity statement. Learning is non-localized, patterns are strengthened between individual neurons throughout the global

region considered- there is no Central Processing Unit. Furthermore, there is no appeal to symbols necessary. Rather than as a rule-driven symbol manipulator, the brain is viewed as "a self-organized process of adaptive interaction with the environment"[10]. However, this speculation on the nature of learning is not confirmed by behavior exhibited by the model. The validity of Freeman's conjecture is an important question. Attaining any answer necessitates further investigation. Indeed, later investigations including "Spacial EEG Correlates of Nonassociative and Associative Olfactory Learning in Rabbits."[9] reveal "no evidence for odor-specific spatial EEG patterning".

Similarly, Freeman's speculations on the functionality of chaotic behavior force open new avenues for further investigation. Freeman writes that "chaotic behavior is essential for":

1) Rapid and unbiased acces to all latent attractors
2) preventing atrophy from disuse
3) eliminating the necessity of an exhaustive search to classify a novel odor
4) allowing a system to escape from its established repertoire of responses in order to add a new response to a novel stimulus under reinforcement.
5) preventing periodic entrainment of neuro-electrical signals that might result in seizure.

Some of these seem more common sense than others, but in none of them is it clear why chaotic behavior is necessarily needed to achieve those functions. Furthermore, it seems that the psychological dimension of the model is still extremely limited, being competent to simulate only pre-attentive cognition. Regardless, it seems that Freeman's method is a definite step up from much of current brain research methodology, genuinely presenting us with "a brain theory that can be tested, elaborated,

or negated by physiological experiments; ... not merely computational."[10]

Works Cited

1 Babloyantz, A., Gallez, D., "Predictability of human EEG: a dynamical approach" Biological Cybernetics, 64 (1991) 381-391.

2 Bressler, S.L. "Relation of olfactory bulb and cortex I", Brain Research, 409 (1987) 285-293.

3 Eckmann, J.P., Ruelle, D., "Liapunov Exponents from time-series", Physical Review A, 34 (1986) 4971-4979.

4 Freeman, W.J., Mass Action in the Nervous System, Academic Press, NY, 1975.

5 Freeman, W.J., "Nonlinear dynamics of paleocortex manifested in olfactory EEG", Biological Cybernetics, 35 (1979) 21-37.

6 Freeman, W.J., "Simulation of Chaotic EEG Patterns with a Dynamic Model of the Olfactory System", Biological Cybernetics, 64 (1991) 381-391.

7 Freeman, W.J., Eeckman F.H., "Assymetric Sigmoid non-linearity in the rat olfactory system", Brain Research, 557 (1991) 13-21.

8 Freeman, W.J., Eeckman F.H., "Correlations between unit firing and EEG in the rat olfactory system.", Brain Research, 528 (1990) 238-244.

9 Freeman, W.J., Grajski, R.A., "Spacial EEG correlation of Nonassociative and Associative olfactory learning in Rabbits", Behavioral Neuroscience, 103:4 (1989) 790-804.

10 Freeman, W.J., Skarda C.A., "How brains make chaos in order to make sense of the world", Behavioral and Brain Sciences, 10 (1987) 161-195.

11 Grassberger, P., "Generalized Dimension of Strange Attractors", Physics Letters A, 97A (1983) 227-230.

12 Rapp, P.E., Zimmerman I.D., "Dynamics of spontaneous neural activity in the simian motor cortex: the dimension of chaotic neurons", Physics Letters A, 110A:6 (1985) 335-338.

13 Searle, J.R., "Conciousness, explanatory inversion, and cognitive science", Behavioral and Brain Sciences, 13:4 (1990) 585-601.

Works Cited

14 Theiler, J., "Testing for nonlinearity in time series: the method of surrogate data", Physica D, 58 (1992) 77-94.